

Intrinsic Limits of Read Trimming in Single-Stranded Bisulfite Sequencing

Yihan Fang^{1*}

¹School of Engineering, Tufts University, 177 College Ave, Medford, 02155, Massachusetts, United States.

Corresponding author(s). E-mail(s): yihan.fang@tufts.edu;

Abstract

Single-stranded whole-genome bisulfite sequencing (ssWGBS) enables DNA methylation profiling in low-input and highly fragmented samples, including cell-free DNA, but introduces stochastic enzymatic artifacts that complicate pre-processing and downstream interpretation. In post-bisulfite library construction, Adaptase-mediated tailing blurs the boundary between biological sequence and synthetic additions, rendering read trimming a persistent source of variability across analytical pipelines. We show that this variability reflects an intrinsic limit of per-read boundary inference rather than an algorithmic shortcoming: boundary localization is fundamentally asymmetric between paired-end reads, with Read 2 exhibiting kinetically structured artifacts that support *constrained* read-level inference, while apparent contamination in Read 1 arises conditionally from geometry-driven read-through events and is not well-defined at the single-read level. Even within Read 2, bisulfite-induced compositional degeneracy creates an indistinguishable regime in which genomic and synthetic origins share support under the same observable sequence evidence, implying a strictly positive Bayes error under any deterministic per-read decision rule and placing a fundamental limit on per-read boundary fidelity. By explicitly characterizing these limits, we reframe read trimming in ssWGBS as a constrained inference problem and introduce a conservative framework that operates only where supported by observable evidence (including short-range nucleotide texture), exposes interpretable trade-offs between genomic retention and residual artifact risk, and avoids forced resolution where boundaries are intrinsically unresolvable. Together, these results clarify why fixed trimming heuristics persist in practice and provide a principled foundation for uncertainty-aware preprocessing in ssWGBS.

Keywords: DNA methylation, single-stranded WGBS, bisulfite sequencing, read trimming, boundary inference, information-theoretic limits, enzymatic tailing, compositional degeneracy

1 Introduction

Single-stranded whole-genome bisulfite sequencing (ssWGBS) enables genome-wide DNA methylation profiling in sample types where conventional double-stranded workflows fail[1], including cell-free DNA and highly fragmented clinical material.[2, 3] These advantages, however, come at the cost of increased preprocessing complexity. In ssWGBS libraries constructed via post-bisulfite chemistry, enzymatic tailing artifacts blur the boundary between biological sequence and synthetic additions, rendering read trimming a nontrivial and often heuristic-driven step in downstream analysis pipelines.[4–7] This motivates a basic question: *what can be inferred about read boundaries from FASTQ-level observables alone?*

Read trimming in ssWGBS is commonly implemented as a uniform, sample-level truncation applied across all reads.[8, 9] Such constant trimming strategies are attractive for their simplicity and robustness to noise, but they implicitly bypass the question of per-read boundary inference. This practice reflects a pragmatic community consensus: while Adaptase-mediated extensions are known to be stochastic and chemistry-dependent, robust per-read localization is often not reliably justified from pre-alignment observables, so pipelines default to a single conservative truncation that stabilizes downstream behavior. What remains unclear, however, is *when* read-level intervention is informationally admissible and *how* trimming decisions should be structured once intrinsic ambiguity is acknowledged.

These considerations raise a more fundamental question: whether a uniquely correct trimming boundary can, in principle, be inferred for individual reads in ssWGBS data. When enzymatic tailing introduces sufficient stochastic variation, local sequence evidence can become statistically indistinguishable from biological sequence, even under idealized assumptions of error-free observation. In this setting, trimming behavior is constrained by limits of observability rather than algorithmic design. Here we formalize this gap by distinguishing (i) contraction of a plausible transition region using aggregate compositional cues from (ii) point-wise boundary recovery, which is generally unsupported in the indistinguishable regime; this motivates decision logic that acts only where evidence is admissible and otherwise defaults to abstention or conservative safeguards. Importantly, these limits do not arise uniformly across reads: library construction and sequencing geometry introduce structural asymmetries between paired-end reads, motivating distinct handling strategies (Fig. 1).

2 Results

Here we show that per-read boundary inference in ssWGBS is fundamentally constrained by the statistical and physical structure of post-bisulfite library construction. We first characterize these constraints at the level of individual reads and aggregated samples, then introduce a trimming framework that acts only where inference is supported and remains conservative where it is not. Finally, we show how making trimming decisions explicit exposes an interpretable retention–purity trade-off and clarifies its downstream biological consequences.

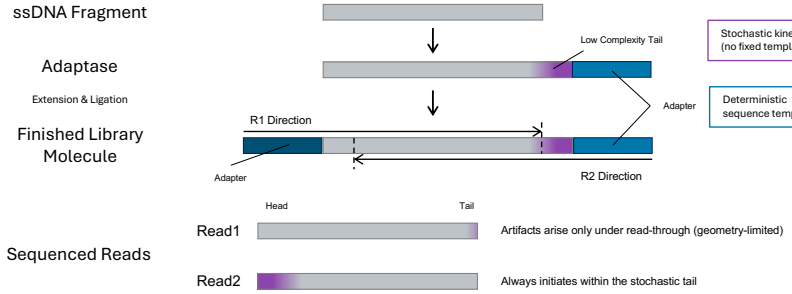


Fig. 1 Physical origin of asymmetric artifacts in ssDNA library preparation. Single-stranded DNA fragments undergo adaptor ligation followed by terminal tailing, producing a finished library molecule with two fundamentally different boundary types. The ligated adaptor constitutes a deterministic sequence template and is typically removed during standard preprocessing, whereas adaptase tailing generates a stochastic kinetic polymer with no fixed template or cut-point. Due to sequencing geometry and variable insert length, Read 2 necessarily initiates within the adaptase-tailed region, while Read 1 contains synthetic sequence only under read-through when the read length exceeds the insert length. This intrinsic asymmetry arises from sequencing geometry, and constrains boundary localization in Read 2 to a region rather than a point, while rendering read-level boundary inference for Read 1 not well-defined, motivating distinct downstream handling strategies.

2.1 Boundary inference in ssWGBS is constrained and asymmetric

In this section, we characterize the empirical and statistical structure that constrains per-read boundary inference in ssWGBS, independent of any specific trimming algorithm. Focusing on how synthetic tailing manifests at both the read and sample levels, we show that while strong compositional signals are present, they constrain boundary localization to an admissible transition *regime* rather than a uniquely identifiable point. We further demonstrate that commonly used sample-level trimming strategies arise as pragmatic responses to this constraint, but are structurally mismatched to the underlying heterogeneity. Together, these observations establish the inferential limits within which any trimming strategy must operate.

2.1.1 Read-level composition reveals constrained transitions

Here, we ask not how accurately a boundary can be predicted, but whether the observable sequence content in individual reads contains sufficient information to support stable per-read boundary inference under realistic ssWGBS conditions. To assess whether per-read boundary inference is supported by the empirical structure of ssWGBS data, we first examined read-level base composition patterns in Read 2 across representative libraries. Read 2 provides a particularly informative setting for this analysis, as synthetic sequence introduced by adaptase tailing is present in the vast majority of reads, independent of insert length or read-through geometry.[4, 7] This allows boundary inference to be evaluated in a regime where artifactual signal is systematic rather than incidental.

Visualization of individual Read 2 sequences revealed a characteristic low-complexity prefix enriched in guanine and adenine, followed by bisulfite-converted

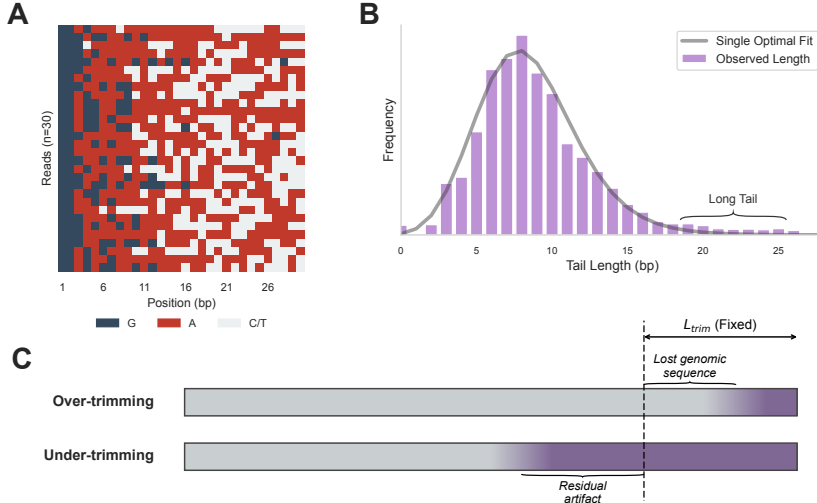


Fig. 2 Read-level heterogeneity and the structural limits of fixed-length trimming in ssWGBS. (A) Base-level composition across 30 representative Read 2 sequences illustrates pronounced read-to-read variability in the transition from enzymatic tailing to genomic sequence. Guanine-rich artifacts (dark) and adenine-enriched bisulfite-converted bases (red) intermix stochastically, producing extended regions where synthetic and biological sequence cannot be reliably distinguished at the single-read level. (B) Distribution of inferred tail lengths shows a unimodal core with a pronounced long tail. A single optimal fit captures the central tendency but systematically fails to explain extreme tailing events, indicating that no unique per-read boundary can be recovered from sequence content alone. (C) Conceptual illustration of fixed-length trimming. A global cut-point inevitably induces over-trimming in reads with shorter tails, resulting in loss of genomic sequence, and under-trimming in reads with longer tails, leaving residual artifacts. Together, these panels show that constant trimming reflects a pragmatic compromise rather than a principled solution, as the true boundary is structurally heterogeneous and not directly observable from individual reads.

genomic sequence (Fig. 2A). Importantly, several strong discriminative signals are consistently present: guanine-rich segments provide a reliable indicator of synthetic tailing, while cytosine depletion and thymine enrichment mark genomic sequence after bisulfite conversion. These signals provide strong discriminative contrast at the aggregate level and allow rapid localization of an approximate transition from synthetic to genomic sequence across reads.

Despite the presence of these strong classifiers, a substantial region of ambiguity persists at the read level. This ambiguity does not arise from feature overlap between synthetic and genomic signals, but from the limited discriminative power of adenine-rich sequence. Adenine is highly prevalent in bisulfite-converted genomic DNA and also constitutes a frequent, though secondary, component of adaptase-generated tails. As a result, extended adenine-enriched regions cannot be cleanly assigned to either class, producing a regime of local configurations in which genomic and artificial origins share support under the same observable evidence, so point-wise boundary recovery is not justified. This limitation persists even under idealized modeling assumptions that assume perfect knowledge of base identity and error-free observation of the sequence content. In this region, the overlap in class-conditional evidence implies a strictly

positive Bayes error, such that no deterministic per-read decision rule can achieve perfect separation (see Supplementary Note 1 for a formal discussion).

More generally, this limitation arises whenever boundary inference relies on observable sequence content drawn from a finite nucleotide alphabet without an orthogonal discriminative marker; *intrinsic indistinguishability between synthetic and genomic sequence is unavoidable, implying a strictly positive Bayes error*, and exact per-read boundary recovery is therefore impossible for a subset of reads, regardless of algorithmic sophistication.

Taken together, these observations indicate that per-read boundary inference in Read 2 is information-rich yet structurally constrained. Strong compositional signals rapidly narrow the candidate boundary region, but intrinsic stochasticity within this evidence-overlap regime prevents stable localization of a unique cut position from local sequence features alone. This structure motivates trimming strategies that treat boundary localization as a constrained inference problem, acting conservatively within an admissible transition regime rather than enforcing deterministic point estimates.

2.1.2 Sample-level constant as a mismatched fallback

Indeed, as shown in Fig. 2B, aggregate tail-length profiles derived from representative ssWGBS libraries exhibit a pronounced central peak accompanied by a long tail. The presence of a dominant mode indicates that, despite substantial read-level heterogeneity (Fig. 2A), many reads cluster around a characteristic trimming range. This structure explains why a single constant cut length can serve as an acceptable engineering fallback in practice, particularly under constraints of robustness and computational simplicity. Accordingly, most existing ssWGBS pipelines implement trimming at the sample level using a fixed constant, which is inexpensive to apply and stable across diverse datasets. [8, 9]

However, the same aggregate distributions also reveal systematic mismatches that limit the effectiveness of constant trimming. First, tail lengths span a broad range, with non-negligible frequency across nearly the entire observed interval, implying that most candidate cut lengths will mis-handle a substantial fraction of reads. Second, the extended tail cannot be adequately captured by a single generative process: distributions that fit the central mode fail to explain extreme tailing events. Together, these properties indicate that constant trimming is structurally mismatched to the underlying variability, even when it appears acceptable at the population level.

This mismatch becomes critical in challenging samples, where the apparent smoothness of the aggregate profile breaks down as a reliable guide. The inferred tail-length distribution spans a wide range and contains a substantial long-tail component (Fig. 2B), such that the population-level operating point itself becomes ambiguous rather than merely suboptimal. Under these conditions, constant trimming ceases to function as a dependable fallback, motivating approaches that make the yield–risk trade-off explicit rather than collapsing it into a single fixed parameter.

2.1.3 Structural consequences of fixed-length trimming

As illustrated conceptually in Fig. 2C, applying a single global cut-point necessarily induces two opposing error modes. Reads with shorter tails are over-trimmed,

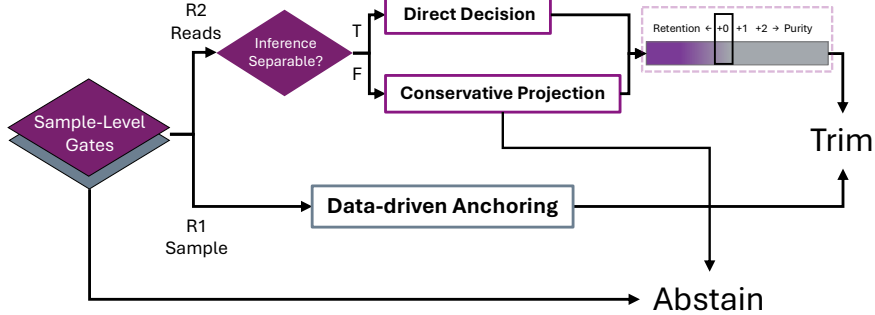


Fig. 3 Adaptive decision flow for read trimming with conservative fallback. Reads first pass sample-level gates to determine whether read-level inference is admissible based on sample-level conditions. For Read 2 (R2), inference separability determines whether a direct operating point can be selected along a continuous retention–purity axis. When inference is not separable, a conservative projection is applied, yielding a guarded trimming decision or abstention. Read 1 (R1) is handled independently via data-driven anchoring at the sample level. Paths leading downward indicate conservative rejection or abstention, ensuring that trimming is only applied when inference is admissible.

resulting in loss of genomic yield, whereas reads with longer tails are under-trimmed, leaving residual synthetic sequence at the 5' end. In ssWGBS, such residual carryover is not merely a technical nuisance. Guanine-rich artifacts retained after trimming can be misinterpreted as methylated cytosines following bisulfite conversion, generating false methylation signal. Constant trimming therefore enforces a structural trade-off between genomic yield and false methylation risk that cannot be resolved by adjusting the cut length alone.

Together, these observations indicate that the limitations of constant trimming arise not from poor parameter choice, but from an inability to adapt trimming behavior to read-level heterogeneity. This motivates trimming strategies that respond to local informational structure where available, while explicitly constraining risk in regions where boundary localization is intrinsically information-limited.

2.2 A physics-informed trimming framework

Motivated by the constrained and asymmetric structure of boundary inference in ssWGBS, we developed a trimming framework that acts only where inference is supported and remains conservative where it is not. Rather than optimizing a single global cut length, the framework separates feasibility assessment from read-level decision-making and explicitly decouples the handling of Read 2 and Read 1 according to their distinct physical origins. By construction, trimming is treated as a conditional decision problem: decisions are applied only when supported by observable sequence evidence and are withheld otherwise. This design exposes the inherent retention–purity trade-off while avoiding forced resolution in regimes where boundary localization is intrinsically information-limited.

2.2.1 Framework overview and read-level gating

The framework is organized as a small number of sequential control steps that regulate when trimming is admissible and how decisions are made (Fig. 3). Before any read-level inference, reads pass through a lightweight sample-level gate that determines whether trimming is warranted at all. This gate functions solely as admission control, preventing unnecessary intervention in samples that are already clean or adequately processed, and does not itself determine trimming boundaries.

A central design principle is the decoupled handling of Read 2 (R2) and Read 1 (R1), reflecting their fundamentally different generative mechanisms. In R2, adaptase-generated sequence is present in the majority of reads and boundary inference is systematically required. In contrast, apparent contamination in R1 arises only conditionally, through the interaction of stochastic tailing and geometry-driven read-through. These processes are statistically independent and give rise to distinct error structures, motivating separate handling strategies rather than a shared trimming rule.

For R2 reads admitted to read-level processing, the framework evaluates inference separability based on the accumulation of observable local sequence evidence rather than fitted models or learned parameters. Here, “local evidence” refers to short-range compositional and transition signatures (e.g., dinucleotide-level texture) induced by kinetic tailing under the specified chemistry. When separability is high, a direct operating point is selected along a continuous retention–purity axis, yielding a localized trimming decision supported by strong compositional contrast. When separability is not supported by the available evidence, non-separable reads are not treated uniformly: reads dominated by weakly informative adenine-rich regions are handled via conservative projection that restricts trimming to a guarded region, whereas reads exhibiting no detectable contamination signal are explicitly left untrimmed through read-level abstention. In all cases, epistemic uncertainty leads to reduced action rather than spurious precision.

To make these behaviors operationally accessible, the framework exposes a small set of discrete operating points that adjust the retention–purity trade-off after inference without altering evidence evaluation. Read 1 is handled differently: because read-level inference is information-limited on average, the framework deliberately falls back to data-driven anchoring at the sample level rather than forcing per-read decisions. While this may resemble constant trimming in form, it differs in that decisions are automatically calibrated to the sample and embedded within the same conservative logic applied to R2.

Importantly, the framework operates independently of read merging and is applied prior to alignment; trimmed reads can be processed with standard bisulfite aligners (e.g., Bismark [10]). Operational integration details and activation-aware runtime measurements are provided in Supplementary Notes 6 and 8.

2.2.2 Inference behavior under controlled uncertainty

We evaluated whether the framework exhibits stable and conservative behavior under controlled perturbations, focusing on regimes where exact boundary recovery is intrinsically ill-defined and modeling assumptions are deliberately violated. Because the

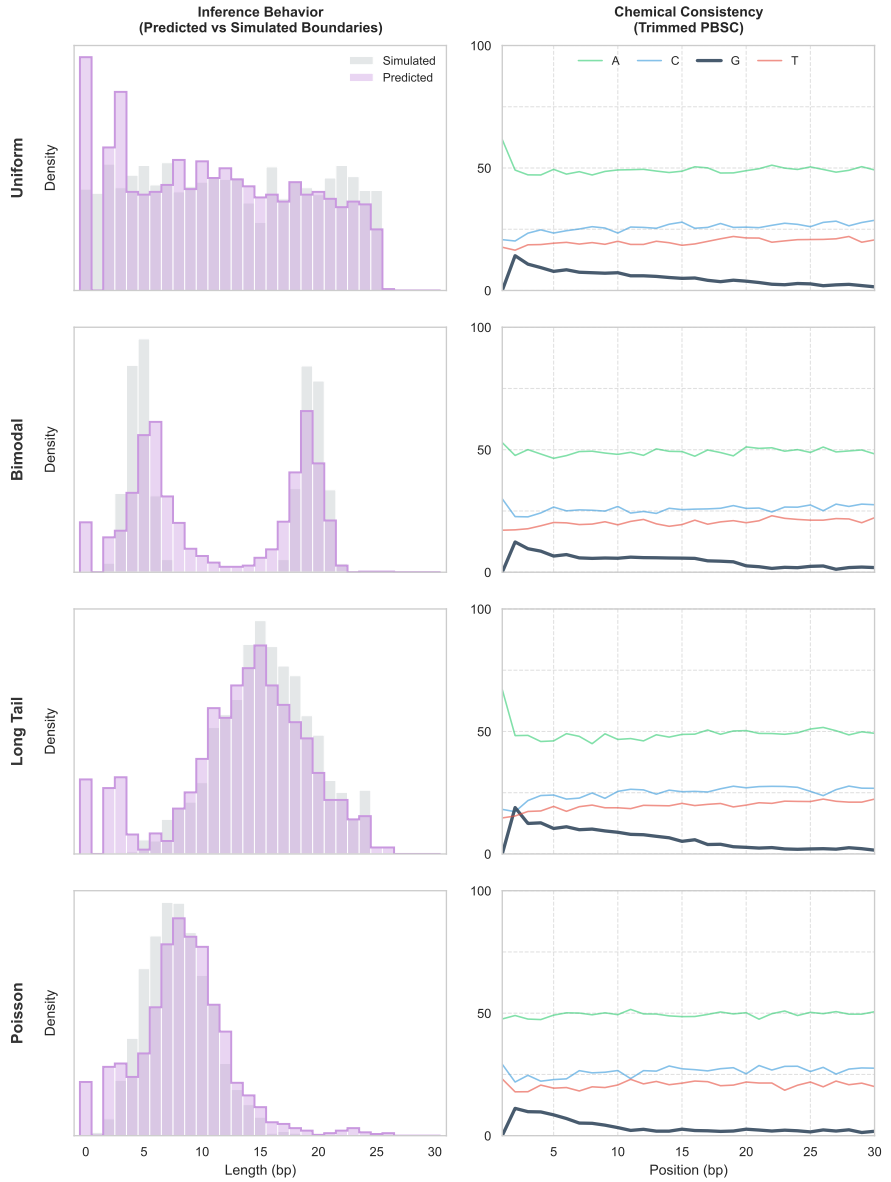


Fig. 4 Inference behavior and chemical consistency under controlled uncertainty. Figure 4 evaluates read-level boundary inference for Read 2 following sample-level gating under controlled synthetic regimes. The left column compares inferred trimming distributions to simulated boundary distributions across four regimes (Uniform, Bimodal, Long Tail, and Poisson), spanning idealized tails and adversarial mixtures that violate modeling assumptions. Agreement in distributional shape, rather than pointwise accuracy, indicates stable inference within regions where exact boundary recovery is intrinsically ill-defined. The right column reports per-base sequence content (PBSC) profiles of trimmed reads, confirming that trimming preserves chemical consistency without introducing systematic compositional bias. Together, these results show that the framework recovers robust structural features while remaining conservative under uncertainty.

primary source of intrinsic ambiguity arises in Read 2, all evaluations target the Read 2 inference branch following sample-level gating, where boundary uncertainty is unavoidable rather than incidental. Synthetic boundary regimes were constructed to span both idealized single-process tails and adversarial mixtures (Supplementary Note 7).

Across all regimes, inferred trimming profiles preserved the overall structural shape of the simulated boundary distributions, including dominant modes and relative ordering of transition regions, even when absolute trimming magnitudes were attenuated under severe perturbation (Fig. 4, left). Rather than enforcing pointwise boundary recovery in intrinsically indistinguishable regions, the framework adaptively reduced trimming aggressiveness as local evidence degraded. Agreement at the distributional level therefore provides a meaningful indicator of stable inference behavior under intrinsic uncertainty.

To assess whether inference-driven trimming introduces chemical distortion, we examined per-base sequence content (PBSC) profiles of trimmed reads (Fig. 4, right). Across all regimes, PBSC profiles remained chemically consistent, with no systematic enrichment indicative of artificial bias. Together, these results show that the framework recovers robust structural features where information permits, constrains action where ambiguity dominates, and preserves chemical plausibility without forcing resolution beyond what the data can support.

2.3 Empirical trade-offs and biological consequences

We next examined how trimming decisions translate into empirically observable trade-offs and downstream biological consequences under the identifiability limits established above. Rather than evaluating trimming strategies solely in terms of boundary recovery, this section focuses on how different operating choices populate the admissible decision space and propagate to biologically meaningful signals. By separating real-data behavior from controlled evaluations, we assess both the structure of this trade-off landscape and its implications for methylation inference.

2.3.1 Explicit trade-offs define an interpretable frontier

Using CCGB-34 (Comprehensive Cell-free & Genomic Bisulfite, $n = 34$), a representative ssWGBS collection spanning both cell-free and genomic DNA, we examined how different trimming strategies populate the empirical decision landscape.[11–17]

For Read 2, adaptive trimming strategies reveal an explicit and navigable trade-off frontier between retained genomic content and residual synthetic signal (Fig. 5A). Varying the deployment offset traverses this frontier from retention-biased to increasingly purity-biased regimes, making the trade-off explicit rather than implicit. Fixed-length trimming and macro-statistical approaches correspond to particular operating points in this landscape: in CCGB-34, a representative constant (10 bp) and the macro-statistical anchor nearly coincide and lie close to the empirical frontier, reflecting that population-level tail statistics can yield a reasonable single-point compromise. However, such points do not expose the admissible frontier itself, nor do they accommodate read-level heterogeneity: they select a single aggregate operating

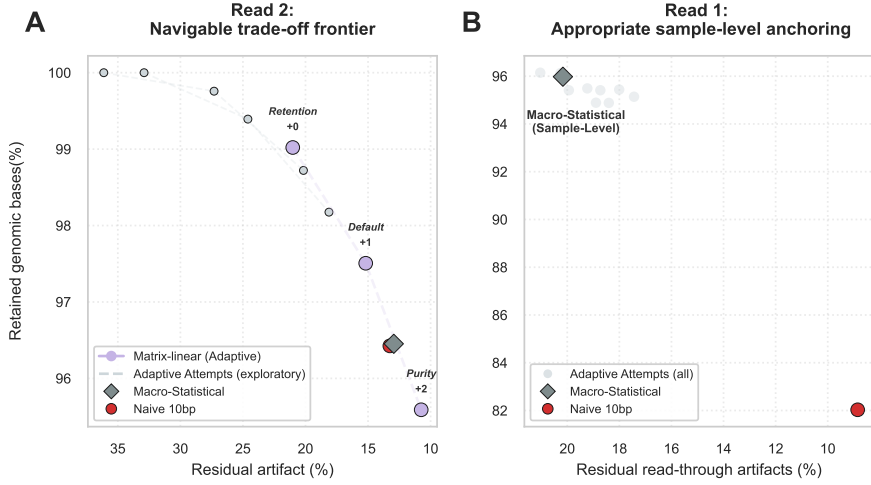


Fig. 5 Asymmetric decision landscapes for Read 2 and Read 1 trimming. (A) For Read 2, adaptive trimming strategies collectively reveal a navigable trade-off frontier between residual synthetic artifacts and retained genomic bases. Exploratory adaptive attempts (grey) delineate the empirically admissible region, while the matrix-linear interface (purple) exposes a small number of interpretable operating points (+0, +1, +2) along this frontier. Fixed-length trimming (red) and macro-statistical trimming (dark grey) correspond to settled aggregate operating points within this space, rather than explicit exploration of the frontier itself. Retention values reflect effective genomic bases retained under admissible inference, rather than absolute biological recovery. (B) For Read 1, adaptive attempts do not form a coherent frontier and instead collapse into an unstructured family (light grey), reflecting an information-limited regime at the read level. In this setting, sample-level anchoring via a macro-statistical constant (dark grey) remains appropriate, while fixed-length trimming (red) represents a rigid but commonly used industrial fallback. Together, these panels show that adaptivity enables principled navigation of the decision space for Read 2, whereas for Read 1 the decision space itself is non-navigable, motivating fundamentally different trimming strategies for the two reads.

point rather than enabling principled navigation across retention–risk regimes when such navigation is feasible. In contrast, adaptive inference makes the full frontier explicit and allows operating points to be chosen with a clear interpretation in terms of retention–purity trade-offs.

For Read 1, the same analysis yields a qualitatively different outcome (Fig. 5B). Adaptive attempts do not form a coherent frontier but instead collapse into an unstructured family, reflecting the information-limited nature of read-level inference for this read. Apparent contamination in Read 1 arises only conditionally, through the interaction of read-through events and the same tailing process that dominates Read 2, leading to a regime where meaningful trade-offs cannot be resolved at the per-read level. In this setting, sample-level anchoring remains appropriate, while fixed-length trimming represents a rigid industrial fallback rather than an optimizable decision. Together, these results demonstrate that adaptive trimming enables principled navigation of the decision space for Read 2, whereas for Read 1 the decision space itself is effectively non-navigable, necessitating fundamentally different handling strategies.

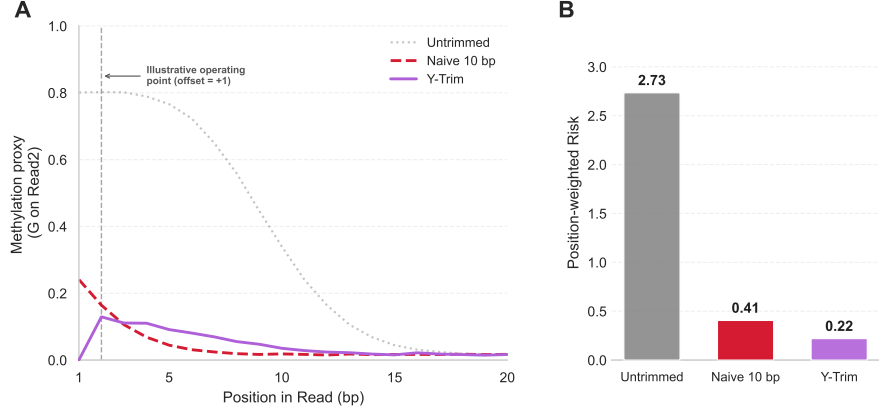


Fig. 6 Position-wise instability profile and 5'-end risk aggregation under an illustrative deployment offset. (A) Read 2 G-content (methylation proxy) across the first 20 bases under three preprocessing choices: untrimmed reads (observational baseline), naive fixed-length trimming (10 bp), and Y-Trim. The dashed vertical line marks an illustrative operating point (offset = +1), which selects a deployment setting after inference rather than altering the underlying decision space. While fixed-length trimming can appear locally competitive at specific early positions, such gains reflect a coincidental alignment with sample-level aggregates imposed by a single global cutoff, rather than stable resolution of heterogeneous read-level behavior. (B) A position-weighted excess-area risk score summarizing 5'-end instability, computed as a rectified deviation above a genomic reference G level with exponentially decaying weights toward the read interior. Under the default aggregation shown here, Y-Trim reduces the integrated 5'-end risk relative to naive trimming, despite not dominating at every position.

2.3.2 CpG-associated methylation inference amplifies early trimming errors

To examine how early trimming errors propagate into downstream methylation-relevant risk under constrained observability, we evaluated trimming outcomes using a CpG-associated [18], position-sensitive proxy. This proxy reflects how small compositional perturbations at the 5' end can be disproportionately amplified during methylation inference [19], without requiring explicit biological labels or region-specific enrichment (Fig. 6). While fixed-length trimming can appear locally competitive under position-wise evaluation across a narrow range of early positions, this behavior largely reflects a rigid leftward shift of the untrimmed baseline rather than stable resolution of read-level heterogeneity. Such apparent gains are therefore not representative of worst- or average-case behavior for fixed-length trimming across samples.

When aggregated across positions, residual guanine-rich artifacts retained after under-trimming contribute to elevated false methylation signal, whereas over-trimming leads to loss of informative genomic sequence. The position-weighted risk profile highlights that these effects accumulate nonlinearly near the read boundary, where early compositional errors exert disproportionate influence on downstream methylation-relevant metrics. In contrast, adaptive trimming reduces integrated 5'-end risk by constraining aggressive decisions in ambiguous regions, even when it does not dominate fixed-length trimming at every individual position. These results underscore that

conservative handling under uncertainty is essential for limiting downstream interpretive risk, and that local performance advantages do not necessarily translate into reliable methylation inference.

3 Discussion

Read trimming in ssWGBS is commonly evaluated using downstream proxies such as read retention or yield. Our results show that these metrics are not reliable indicators of sensitivity in post-bisulfite libraries, where chemically indistinguishable artifacts can inflate apparent retention without adding biological signal. In this setting, the search for a globally “optimal” trimming rule through greedy or black-box optimization is misplaced, because per-read boundary assignment is information-limited rather than under-modeled. Consequently, different trimming strategies are not always meaningfully comparable under a single benchmark. Accordingly, comparisons should be made in terms of chemistry-consistent aggregate criteria rather than pointwise boundary accuracy. More broadly, this shifts the objective of trimming from maximizing nominal yield to controlling downstream interpretive risk under constrained observability. Under post-bisulfite chemistries, the relevant question is not whether a boundary can be estimated precisely, but whether the observable sequence texture contains sufficient evidence to justify irreversible intervention.

Rather than attempting to overcome this limit, our results clarify how trimming decisions must be structured once the full generative process is acknowledged. Read 2 and Read 1 arise from distinct physical mechanisms and therefore admit fundamentally different inferential regimes. In Read 2, synthetic sequence is systematic and inference is unavoidable but bounded, making it meaningful to reason about admissible decision regions. In Read 1, contamination is sparse, geometry-driven, and dominated by a large mass at zero (conditional), placing it in an information-limited regime where per-read adaptivity offers little leverage. These differences motivate a staged formulation in which feasibility is assessed before inference, and inference is applied only where marginal information gain remains meaningful.

Under such constraints, trimming cannot be safely cast as a black-box optimization problem. When pointwise optimality is unattainable, opaque precision risks turning irreducible uncertainty into unquantified bias. These properties are operationalized via gating, abstention, and conservative projection (Supplementary Notes 2–4, 6). Conservatism therefore requires that inference logic be explicit, decision boundaries interpretable, and deployment choices parameterized rather than hidden. In this framework, adjustable operating points are not tuning conveniences but explicit statements of acceptable risk–yield trade-offs under uncertainty. By exposing these choices directly, the framework allows trimming behavior to be reasoned about in relation to downstream consequences, without assuming resolution where the data provide none.

A useful way to view this framework is as *texture-driven decision-making* rather than template matching. In post-bisulfite single-stranded libraries, the dominant artifacts are not defined by a fixed sequence identity, but by a stochastic kinetic process whose footprint appears as short-range nucleotide texture. Accordingly, Y-Trim operationalizes read-level feasibility through deterministic evidence accumulation over local

transition structure (Supplementary Note 3), and treats inference breakdown as a first-class outcome handled by abstention and conservative projection (Supplementary Note 4), rather than forcing point estimates in entropy-dominated regimes.

Crucially, this perspective is not specific to ssWGBS. Many sequencing artifacts are *template-free* but *texture-defined*: they share support with genuine biological sequence under the same nucleotide alphabet, yet exhibit reproducible local statistical signatures induced by platform chemistry or library kinetics. In such settings, per-read preprocessing is inherently constrained by a non-zero error floor (Supplementary Note 1), and robust behavior requires making uncertainty explicit—acting only where evidence is admissible and otherwise defaulting to non-intervention or conservative safeguards. This principle naturally extends to other textured artifacts such as Poly-G tails arising in two-color chemistry systems, where the artifact is not reliably localized by a single deterministic cut-point but remains recognizable through low-complexity texture at the read boundary.

Finally, our evaluation strategy reflects the same philosophy. Because per-read ground truth is not observable in real ssWGBS data, downstream evaluation cannot rely on point-wise correctness, but must operate on chemistry-consistent aggregate summaries. We therefore assess trimming behavior through position-wise base composition profiles and integrated 5'-end risk, which capture how early compositional perturbations propagate into methylation-relevant signal. This perspective treats preprocessing as a problem of controlling downstream risk under constrained observability, rather than recovering unobservable boundaries.

4 Conclusion

Single-stranded bisulfite sequencing enables methylation profiling in low-input and fragmented samples, but introduces stochastic enzymatic artifacts that impose intrinsic limits on per-read boundary inference. These limits arise from bisulfite-induced compositional degeneracy interacting with adaptase tailing, producing an indistinguishable regime with a strictly positive Bayes error, in which genomic and artifactual origins share support under the same observable evidence and perfect read-level separation is unattainable in principle. This structure explains both the persistence of sample-level constant trimming as a pragmatic engineering fallback and its systematic mismatch to the heterogeneous, long-tailed variability observed in practice. By making these limits explicit, our work reframes read trimming in ssWGBS as a constrained inference and decision problem, and establishes a principled foundation for uncertainty-aware preprocessing that prioritizes controllable downstream risk over ill-defined notions of per-read optimality under current post-bisulfite chemistries. More broadly, this establishes an uncertainty-aware preprocessing principle for template-free but texture-defined sequencing artifacts, where admissible action is dictated by observable evidence rather than forced boundary recovery.

Supplementary information. Supplementary Notes, figures, and tables providing detailed methodological descriptions, controlled evaluations, and additional analyses are available with this article.

Acknowledgements. We are deeply grateful to Prof. Lenore Cowen for sustained mentorship, critical guidance on research direction and positioning, and extensive feedback throughout the development of this work. We are grateful to Dr. Yongkun Ji for discussions that clarified the ssWGBS chemistry and pipeline context, and for feedback that improved domain framing and technical conventions. We thank Dr. Rebecca Batorsky for detailed feedback on validation strategy and presentation, and for emphasizing the importance of evaluating downstream biological consequences during method development. We thank Jindan Huang for valuable advice on research planning and publication strategy. We thank Dr. William White for helpful discussions, broader scientific feedback, and advice on manuscript presentation. We thank Prof. Jivko Sinapov for early developmental discussions and algorithmic perspective. We also thank Dr. Albert Tai for technical discussions regarding sequencing workflows, as well as Hiu Mai and Yijia Zhang for preliminary literature exploration.

Declarations

Funding This work was conducted without external grant funding. Publication-related costs are supported through institutional open access resources.

Competing interests The authors declare no competing interests.

Ethics approval and consent to participate Not applicable.

Consent for publication Not applicable.

Data availability All sequencing datasets analyzed in this study are publicly available from NCBI repositories (GEO/SRA/BioProject). The CCGB-34 cohort (Comprehensive Cell-free & Genomic Bisulfite; $n = 34$) was assembled from seven published studies and associated accessions: GSE178666/SRP325062 [11], GSE307705/SRP619043 [12], SRP299418 [13], GSE249140/SRP475142 [14], PRJNA1162448/SRP533334 [15], PRJNA1348139/SRP636882 [16], and PRJNA1328772/SRP620537 [17]. Simulator-generated data and all analysis outputs are reproducible from the code and configuration files provided in the accompanying reproducibility package. (See Code Availability) No new sequencing data were generated for this study.

Materials availability Not applicable.

Code availability

A complete reference implementation of Y-Trim (core inference engine, simulator, demo, and full figure-reproduction workflows) is available for peer review via a view-only OSF link: https://osf.io/etqrj/overview?view_only=795c81dbfa8a4f7185b1c45310628591. The package includes scripts to reproduce all analyses and figures reported in the manuscript. Upon acceptance, the code will be released publicly under the MIT License, and an archived release will be deposited in a long-term repository (e.g., Zenodo or OSF).

Author contributions Y.F. conceived the project, developed the theoretical framework and algorithms, performed all computational analyses, and wrote the manuscript.

References

- [1] Lister R, Pelizzola M, et al. Human DNA methylomes at base resolution show widespread epigenomic differences. *Nature*. 2009;462(7271):315–322. <https://doi.org/10.1038/nature08514>.
- [2] Luo H, Wei W, et al. Liquid Biopsy of Methylation Biomarkers in Cell-Free DNA. *Trends in Molecular Medicine*. 2021;27(5):482–500. <https://doi.org/10.1016/j.molmed.2020.12.011>.
- [3] Zeng H, He B, Yi C, Peng J. Liquid biopsies: DNA methylation analyses in circulating cell-free DNA. *Journal of Genetics and Genomics*. 2018;45:185–192. <https://doi.org/10.1016/j.jgg.2018.02.007>.
- [4] Miura F, Enomoto Y, Dairiki R, Ito T. Amplification-free whole-genome bisulfite sequencing by post-bisulfite adaptor tagging. *Nucleic Acids Research*. 2012;40(17):e136. <https://doi.org/10.1093/nar/gks454>.
- [5] Miura F, Shibata Y, Miura M, Sangatsuda Y, Hisano O, Araki H, et al. Highly efficient single-stranded DNA ligation technique improves low-input whole-genome bisulfite sequencing by post-bisulfite adaptor tagging. *Nucleic Acids Research*. 2019;47(15):e85. <https://doi.org/10.1093/nar/gkz435>.
- [6] Swift Biosciences. Accel-NGS® 1S Plus and Methyl-Seq: Tail Trimming for Better Data. Swift Biosciences; 2015. Accessed via Gene Target Solutions. Available from: <https://www.genetargetsolutions.com.au/wp-content/uploads/2015/05/Accel-NGS%20AE-1S-Plus-Methyl-Seq-Tail-Trimming-For-Better-Data-1.pdf>.
- [7] Swift Biosciences. Tail Trimming for Better Data: Accel-NGS® Methyl-Seq, Adaptase Module and 1S Plus DNA Library Kits. Swift Biosciences; 2019. Accessed via Bioscience. Available from: <https://www.bioscience.co.uk/userfiles/pdf/16-0853-Tail-Trim-Final-442019.pdf>.
- [8] Martin M. Cutadapt removes adapter sequences from high-throughput sequencing reads. *EMBnetjournal*. 2011;17(1):10–12. <https://doi.org/10.14806/ej.17.1.200>.
- [9] Krueger F, James F, Ewels P, Afyounian E, Schuster-Boeckler B.: Trim Galore! Version 0.6.7.
- [10] Krueger F, Andrews SR. Bismark: a flexible aligner and methylation caller for Bisulfite-Seq applications. *Bioinformatics*. 2011 Jun;27(11):1571–1572. <https://doi.org/10.1093/bioinformatics/btr167>.

- [11] Li J, Huang Y, Li X.: Cerebrospinal fluid cell-free DNA methylomes recapTURE pediatric medulloblastoma tissue's tumor feature. NCBI GEO. Accession: GSE178666 / SRP325062. Available from: <https://www.ncbi.nlm.nih.gov/geo/query/acc.cgi?acc=GSE178666>.
- [12] Caggiano C, Morselli M, Qian X, et al. Epigenetic profiles of tissue informative CpGs inform ALS disease status and progression. *Genome Medicine*. 2025;17(1):115. Data available at GSE307705 / SRP619043. <https://doi.org/10.1186/s13073-025-01542-5>.
- [13] Cheng AP, Donnelly S, Queen K, et al. Cell-free DNA profiling of critically ill COVID-19 patients reveals tissue damage and virus footprints. *Cell Reports Medicine*. 2021;2(10):100428. <https://doi.org/10.1016/j.xcrm.2021.100428>.
- [14] Lo EKW, Idrizi A, Tryggvadottir R, et al. DNA methylation memory of pancreatic acinar-ductal metaplasia transition state altering Kras-downstream signaling. *Genome Medicine*. 2025;17(1):32. Data available at GSE249140 / SRP475142. <https://doi.org/10.1186/s13073-025-01542-x>.
- [15] Children's Mercy Research Institute.: Methylation patterns of the nasal epigenome of hospitalized SARS-CoV-2 positive patients. NCBI BioProject. Accession: PRJNA1162448 / SRP53334. Available from: <https://www.ncbi.nlm.nih.gov/bioproject/PRJNA1162448>.
- [16] University of Heidelberg.: Chamber-Specific Chromatin Architecture Guides Functional Interpretation of Disease-Associated Cis-Regulatory Elements. NCBI BioProject. Accession: PRJNA1348139 / SRP636882. Available from: <https://www.ncbi.nlm.nih.gov/bioproject/PRJNA1348139>.
- [17] Quintanal-Villalonga A, Taniguchi H, et al. Multiomic Analysis of Lung Tumors Defines Pathways Activated in Neuroendocrine Transformation. *Cancer Discovery*. 2021;11(12):3028–3047. <https://doi.org/10.1158/2159-8290.CD-20-1863>.
- [18] Deaton AM, Bird A. CpG islands and the regulation of transcription. *Genes & Development*. 2011;25(10):1010–1022. <https://doi.org/10.1101/gad.2037511>.
- [19] Siegfried Z, Simon I. DNA methylation and gene expression. *WIREs Systems Biology and Medicine*. 2010;2(3):362–371. <https://doi.org/10.1002/wsbm.64>.
- [20] Dai Q, Ye C, Irkliyenko I, Wang Y, Sun HL, Gao Y, et al. Ultrafast bisulfite sequencing detection of 5-methylcytosine in DNA and RNA. *Nature Biotechnology*. 2024;42(10):1559–1570. <https://doi.org/10.1038/s41587-023-02034-w>.
- [21] Andrews S.: FastQC: A quality control tool for high throughput sequence data. Babraham Bioinformatics. Available from: <https://www.bioinformatics.babraham.ac.uk/projects/fastqc/>.

- [22] Chen S. fastp: An ultra-fast all-round tool for FASTQ data quality control and preprocessing. *iMeta*. 2025;4(5):e70078. <https://doi.org/10.1002/imt2.70078>.
- [23] Hilbe JM. Negative Binomial Regression. Cambridge University Press; 2011.

Supplementary Materials

The Supplementary Information provides theoretical, operational, and empirical details that support the interpretation of the main text without expanding its narrative scope. Rather than introducing additional performance claims, it clarifies the physical and statistical limits that constrain per-read boundary inference in post-bisulfite ssWGBS data, and documents how the proposed framework is designed to operate within those limits.

Throughout the Supplement, properties of the data-generating process are explicitly separated from algorithmic responses, and decision prerequisites are distinguished from decision mechanisms and their downstream consequences. The framework is described with an explicit emphasis on epistemic restraint: algorithmic actions are limited to information that is directly observable and discriminative at the per-read level, while signals whose apparent utility arises only from aggregation or expectation are deliberately not exploited for per-read boundary placement.

The Supplement is organized into focused notes covering (i) physical and information-theoretic constraints imposed by bisulfite chemistry and enzymatic tailing, (ii) operational definitions governing sample-level admission, read-level inference, abstention, and fallback behavior, and (iii) controlled evaluations that assess behavioral consistency under stress, including synthetic perturbations and biologically motivated risk aggregation. A scenario-based evaluation surface (CCGB-34) is described to contextualize empirical behavior across diverse regimes, together with engineering considerations relevant to practical deployment.

5 Supplementary Note 1: Physical and Information-Theoretic Limits of Boundary Inference in ssWGBS

Overview

This Supplementary Note establishes the physical and information-theoretic constraints that govern boundary inference in post-bisulfite single-stranded whole-genome bisulfite sequencing (ssWGBS). Rather than describing any specific trimming algorithm, the focus here is on the structure of the observable data itself: what information is available at the read level, how that information arises from library chemistry and sequencing geometry, and why certain inference tasks are fundamentally ill-posed regardless of model sophistication. These limits are not merely algorithmic. While bisulfite-based chemistries are also known to induce DNA damage and reduce effective sequence complexity [20], the identifiability limits discussed here arise even under idealized assumptions of error-free observation, and follow directly from shared support of the observable nucleotide alphabet under post-bisulfite chemistry.

The purpose of this note is to separate properties of the data-generating process from algorithmic responses. In particular, it clarifies why per-read boundary localization is intrinsically uncertain in ssWGBS, and why trimming decisions can at best contract a plausible region rather than identify a uniquely correct cut position.

5.1 Observable sequence information and pipeline context

What is observable at the read level.

In ssWGBS preprocessing, boundary inference operates on raw sequencing reads represented as FASTQ records. At this stage, the primary observable information consists of nucleotide identities along each read, together with their positional ordering. Summary statistics such as per-base sequence content (PBSC) profiles provide population-level views of this information by aggregating base frequencies across reads at corresponding positions. PBSC-style summaries are commonly reported in standard FASTQ quality-control outputs (e.g., the “Per base sequence content” module in FastQC). [21]

Importantly, the analysis in this work deliberately restricts itself to information that is directly observable from the sequence itself. Base quality scores, alignment context, read pairing geometry, fragment overlap, and reference-genome consistency are not assumed to be available or reliable at the trimming stage. This restriction reflects both practical pipeline constraints and a conceptual boundary: trimming decisions are made before alignment and should not depend on downstream interpretive layers that already presume the removal of synthetic sequence.

Position of trimming within sequencing pipelines.

In typical ssWGBS workflows, trimming is performed early in the preprocessing pipeline, prior to alignment and independent of read merging. Although some pipelines perform adapter trimming after read merging or use alignment feedback to guide

trimming heuristics, such approaches implicitly rely on assumptions about fragment reconstruction that are not uniformly valid for low-input or highly fragmented libraries.

The framework analyzed here treats trimming as a pre-alignment operation that acts independently on individual reads. As a result, boundary inference must rely solely on local sequence texture rather than global consistency checks, and any uncertainty inherent in the observable sequence cannot be resolved by deferring decisions to later pipeline stages.

5.2 From observable texture to empirical ambiguity

Local compositional signals and their limits.

At the level of individual reads, post-bisulfite ssWGBS data exhibit strong local compositional structure. Synthetic sequence introduced during library preparation often shows low complexity and biased nucleotide composition, while bisulfite-converted genomic DNA displays characteristic depletion of cytosine and enrichment of thymine. These signals provide clear evidence that synthetic and biological sequence are, in aggregate, distinguishable.

However, this distinguishability is not uniform across all positions or all reads. Certain nucleotides occur with substantial frequency in both synthetic extensions and bisulfite-converted genomic sequence. As a result, local sequence texture can be informative in some regions while becoming weakly discriminative in others, particularly near the transition between synthetic and genomic segments.

Shared support rather than a spatial cut-point.

Ambiguity in ssWGBS trimming does not arise from an unknown physical cut-point along the read, but from shared support of observable sequence configurations under both genomic and artifactual generative processes. That is, there exist local sequence contexts for which both genomic and artifactual origins assign non-zero probability given the same observable evidence.

We refer to this regime as an *indistinguishable zone*: a class of local sequence configurations for which both genomic and artifactual origins are statistically plausible under the same observable evidence, due to bisulfite-induced compositional degeneracy. In this zone, deterministic separation of individual reads is statistically infeasible, regardless of algorithmic strategy. The term is used descriptively rather than as a formally delineated region; it denotes the existence of overlapping evidence rather than a spatially localized boundary along the read.

Consequences for boundary localization.

The existence of an indistinguishable zone implies that per-read boundary inference can at best contract a plausible transition region rather than identify a unique cut position. While strong compositional signals can rapidly exclude large portions of the read from consideration, the remaining candidate region cannot be resolved to a single point using sequence texture alone.

This limitation persists even under idealized assumptions of error-free base calling and perfect knowledge of population-level base frequencies. It is therefore a property of the observable data itself, not a consequence of noise, insufficient training data, or suboptimal modeling.

This irreducible ambiguity is reflected indirectly in engineering practice. Early technical guidance for Adaptase-based ssWGBS libraries proposed fixed trimming lengths (e.g., 10 bp) as conservative engineering heuristics to suppress dominant synthetic signal, without explicitly modeling per-molecule tail-length variability. [6] Subsequent revisions increased the recommended fixed trimming length (e.g., to 15 bp) and supplemented these heuristics with empirical summaries of tail extent. In particular, later documentation reported a median synthetic tail length on the order of 8 bp as an operational summary, reflecting accumulated experience rather than a change in the underlying identifiability limits. [7] These revisions should therefore be understood as pragmatic engineering responses to persistent ambiguity, rather than as evidence that the underlying identifiability limits can be resolved.

Importantly, such adjustments do not resolve the underlying identifiability problem. Rather, they represent heuristic responses to the same indistinguishable zone described above: as experience accumulates, fixed cutoffs are shifted to reduce average residual artifact, at the cost of additional genomic sequence loss. The need for revision itself underscores that no single deterministic cut position can be justified at the per-read level from observable sequence texture alone.

5.3 Irreducible Bayes error under bisulfite chemistry

Single-read inference as a binary classification problem.

Per-read boundary inference can be framed as a sequence of binary classification decisions: at each position, the observed local sequence context is assigned either to genomic origin or to synthetic extension. Each decision is made on the basis of a finite local observation drawn from distributions induced by library chemistry and bisulfite conversion. This framing is used solely to reason about limits of separability, not to suggest that trimming is implemented as an explicit classifier.

Population-level summaries such as PBSC profiles implicitly assume an i.i.d. generative process within each region. At the level of individual reads, however, only a single realization from this process is observed. As long as the class-conditional distributions over observable features overlap, no deterministic rule can guarantee correct classification for all reads.

Overlap implies a non-zero error lower bound.

The key implication of this overlap is the existence of a strictly positive Bayes error: a lower bound on the probability of misclassification that cannot be eliminated by improved modeling or additional computation. In ssWGBS, this overlap arises because certain nucleotides and short motifs occur with non-zero probability in both synthetic extensions and bisulfite-converted genomic DNA.

Adenine-rich sequence provides a canonical example of this phenomenon, but the argument is not specific to adenine. Any nucleotide or motif that is shared between

the two generative processes necessarily induces overlap in feature space and enforces a positive error floor.

Chemistry dependence without full separability.

Different library chemistries can shift the degree of overlap by altering the relative frequencies of nucleotides in synthetic extensions. In principle, a hypothetical chemistry producing a perfectly exclusive synthetic alphabet could reduce ambiguity. In practice, all current chemistries generate synthetic sequence composed of the same nucleotide alphabet as genomic DNA, differing only in relative composition.

As a result, while chemistry choice influences the *extent* of the indistinguishable zone, it does not eliminate it. As long as genomic DNA assigns non-zero probability to the same bases, per-read boundary inference is subject to irreducible Bayes error under base-level observation.

Implications for trimming strategies.

The presence of irreducible Bayes error implies that any approach enforcing a single, deterministic cut position at the per-read level assumes separability that the data do not support. Such approaches may appear effective on average but will necessarily incur systematic errors on subsets of reads drawn from the indistinguishable regime.

Conversely, trimming strategies that acknowledge this limit can aim to confine decisions to regions where marginal information gain remains meaningful, and refrain from forced resolution once local evidence becomes entropy-dominated. In this sense, the goal of trimming is not to recover an unobservable boundary, but to manage uncertainty in a way that minimizes irreversible downstream harm.

6 Supplementary Note 2: Sample-Level Admission — Gating, Activation, and “Dirty Sample” Semantics

Overview

This Supplementary Note defines the *sample-level admission logic* that determines whether trimming analysis is activated at all. Gating in this context does *not* perform boundary inference and does *not* determine cut positions. Instead, it functions as a feasibility constraint, ensuring that downstream trimming decisions are attempted only when the observable evidence supports meaningful intervention. In other words, gating is designed to identify samples in which read-level inference is informationally admissible, rather than to conservatively reject marginal cases.

Throughout, we separate *activation* from *inference*. Activation answers: “*Is trimming admissible for this sample under the available information?*” Inference (described in later Notes) answers: “*Where should trimming occur when admissible?*” This separation prevents forced resolution in regimes where local evidence is intrinsically limited.

6.1 Observable information and non-intervention principle

All admission decisions are based exclusively on information directly observable from raw sequencing output. Y-Trim operates on per-base sequence content (PBSC) profiles computed from FASTQ files, which summarize base frequencies as a function of read position under random sampling of reads. No alignment, read-pair merging, fragment reconstruction, or quality-score filtering is assumed or required.

PBSC aggregation is strictly descriptive: it does not alter read-level randomness, and it does not condition or bias downstream analysis. Its purpose is to expose systematic deviations in base composition near read boundaries that are otherwise obscured by stochastic variation at the level of individual reads.

Operationally, trimming is positioned prior to alignment and independent of read merging. Some workflows apply trimming after read merging; Y-Trim explicitly avoids assumptions about insert reconstruction, so that admission decisions remain decoupled from downstream pipeline ordering.

6.2 Gating as admission control, not detection

Sample-level gating is intentionally conservative. Its role is not to detect contamination exhaustively, but to prevent irreversible trimming actions in samples where evidence is weak, inconsistent, or dominated by noise. A sample that fails gating is not declared “biologically clean”; it is deemed *inadmissible* for trimming inference under the available information.

Accordingly, gating is designed to favor specificity over sensitivity. False negatives (abstaining on a mildly contaminated sample) are tolerated, whereas false positives (trimming under fundamentally ambiguous evidence) are explicitly avoided.

6.3 Read 2 gating: kinetic admissibility under dominant-G chemistry

For Read 2, gating exploits the characteristic kinetic signature introduced by Adaptase-mediated tailing. In the ssWGBS regimes considered here, synthetic extensions are dominated by **guanine** with adenine as a secondary component. Adenine-rich sequence is intrinsically ambiguous in bisulfite-converted genomic DNA and contributes to the indistinguishable regime (Supplementary Note 5). Guanine, by contrast, provides the most robust chemistry-consistent discriminative anchor because its genomic baseline near the read start is low under post-bisulfite conversion.

Read 2 gating is therefore driven by guanine-centered PBSC structure rather than absolute thresholds. Within a fixed early window, the gate evaluates whether the PBSC profiles exhibit an *ordered set of heterogeneous crossovers* originating from guanine (i.e., the first $G \rightarrow A$ crossover occurs early and is accompanied by at least one additional heterogeneous crossover such as $G \rightarrow C$ or $G \rightarrow T$). Only the relative ordering of the first crossover events is used. Subsequent oscillatory intersections are intentionally ignored, as they are common in low-contrast regimes and do not provide stable admission evidence.

The Read 2 observation window is fixed at $L_{\text{cross}} = 30$ bases. This length is chosen to be longer than the inference horizon used later for per-read stopping, ensuring that

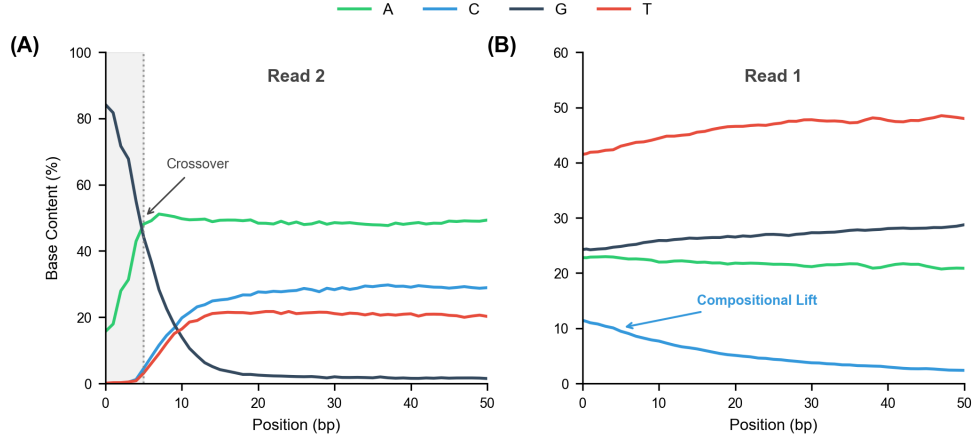


Fig. S1 Asymmetric observability of artifact signals underlying sample-level admission. (A) **Read 2 (kinetically driven).** Adaptase-mediated extension produces a Guanine-enriched synthetic prefix with a secondary Adenine contribution characteristic of the sswGBS regimes analyzed here. After bisulfite conversion, this process yields reproducible aggregate-level compositional crossover structure in practice. These crossovers provide sufficient evidence for *sample-level admission* of Read 2 trimming analysis, but do not imply the existence of a uniquely localizable per-read boundary. (B) **Read 1 (geometry-limited).** Read 1 artifacts arise conditionally through geometry-driven read-through when $L_{\text{read}} > L_{\text{insert}}$, producing a diffuse cytosine lift observable only under aggregation. While compositional intersections may appear in PBSC profiles, their positions are not synchronized across reads and therefore do not support read-level boundary inference. Accordingly, Read 1 signals are used exclusively for feasibility gating rather than point estimation.

admission logic does not depend on downstream inference outcomes. It also allows multiple heterogeneous crossovers to be observed without relying on quantitative magnitude thresholds.

6.4 Read 1 feasibility gating: geometry-limited contamination as a sample property

Read 1 contamination arises only conditionally through geometry-driven read-through when $L_{\text{read}} > L_{\text{insert}}$. As a result, Read 1 artifacts are sparse, positionally unstable, and not synchronized across reads. Per-read boundary inference is therefore ill-posed on average, and Read 1 gating is formulated strictly as a *sample-level feasibility check*.

Read 1 feasibility gating combines two complementary criteria:

Crossover existence as a severe-case shortcut.

Within an early window, the gate checks for the existence of crossover behavior involving cytosine. Positional consistency is not required: under insert-length heterogeneity, crossover locations are not expected to align across reads. The presence of at least one crossover event is treated as a coarse feasibility indicator of strong read-through, and serves as an intuitive shortcut in severe regimes. In principle, a sufficiently detailed lift-based rule could operate without explicit crossover checks; crossover existence

is included because it enables rapid identification of severe geometric regimes with minimal assumptions.

The Read 1 crossover window is restricted to $L_{\text{cross}}^{(R1)} = 15$ bases. This choice reflects a deliberate trade-off: severe read-through tends to manifest early in aggregates, so a shorter window provides a fast, conservative admission shortcut, while avoiding over-reliance on later positions where contrast is lower.

Relative cytosine lift for broad feasibility.

Because Read 1 behavior is dominated by geometry rather than a localized kinetic transition, the primary feasibility signal is a *relative* cytosine lift that is coherent under aggregation. The lift is evaluated against a local baseline rather than as an absolute increase, making the criterion robust to species- and protocol-dependent background composition. To avoid activation driven by high-frequency oscillations (platform jitter) or sampling noise, the lift criterion additionally requires stability under PBSC aggregation and rejects patterns dominated by short-scale fluctuations.

Together, these criteria distinguish geometry-limited Read 1 regimes from both clean samples and purely noisy regimes. Failing Read 1 feasibility gating does not imply the absence of read-through in every molecule; it implies that the sample-level evidence does not justify irreversible Read 1 trimming.

6.5 Chemistry dependence and guanine-centered robustness

Both Read 2 and Read 1 admission logic rely primarily on **guanine-centered** signals rather than adenine. This is intentional: adenine-rich sequence is intrinsically ambiguous in bisulfite-converted genomic DNA and contributes to the indistinguishable regime. By centering gating on guanine-driven evidence, the framework remains robust across Adaptase-like chemistries with a dominant-G tailing bias (with secondary A contribution), without requiring retuning.

6.6 Scope of this Note

This Note defines admission semantics and the observational basis of gating. Empirical activation rates and scenario-specific gating behavior (including CCGB-34 summaries) are reported separately in the scenario-based evaluation Note, and are not required for the definitions presented here.

7 Supplementary Note 3: Deterministic Read 2 Boundary Inference under Information Constraints

Scope and role of this Note

This Supplementary Note defines the per-read boundary inference mechanism applied to Read 2 (R2) in Y-Trim after sample-level admission has been satisfied (Supplementary Note 6). Its purpose is to specify the deployed decision rule, the evidence aggregation scheme, and the stopping logic governing R2 trimming, without introducing additional performance claims or alternative models.

Table S1 Recommended parameter configuration for sampling and sample-level gating.

Category	Parameter	Setting
Sampling	Minimum sample size (N_{\min})	1,000 reads (any contiguous subset)
	Recommended sample size (N_{rec})	5,000 reads (random subsample)
R2 gating	PBSC window length (L_{PBSC})	30 bp
	Required crossover types	$G \rightarrow X, X \in \{A, C, T\}$
	Ordering constraint	$\arg \min_X \text{pos}(G \rightarrow X) = A$
R1 feasibility	Severe read-through crossover	$C \rightarrow X (X \neq C)$ within positions 0–15
	PBSC window length (L_{PBSC})	30 bp
	Background reference (C_{bg})	Mean C frequency over positions 10–30 (fallback = 0)
	Early inspection window (L_{early})	8 bp
	High-C screening threshold	$C \geq \max(C_{\min}, C_{\text{bg}} + C_{\min})$, $C_{\min} = 4\%$
	Lift confirmation criterion	End-half mean (4 bp) \geq inner-half mean (4 bp) +1%

All inference described here operates exclusively on observed nucleotide sequence content. No base quality scores, alignment-derived signals, or fragment-level reconstruction are used. The procedure is deterministic once the sequencing chemistry is fixed.

7.1 Inference as evidence accumulation, not boundary recovery

R2 carries the direct kinetic footprint of Adaptase-mediated tailing and exhibits substantial molecule-to-molecule variability. Under long-tailed regimes, no fixed positional heuristic can reliably capture this variability at the level of individual reads. Y-Trim therefore formulates R2 trimming as a constrained decision problem driven by cumulative local evidence, rather than as an attempt to recover a unique physical boundary.

For each read, candidate cut positions are evaluated sequentially from the 5' end. At each position, local nucleotide texture is converted into incremental evidence supporting either synthetic tailing or genomic sequence. Evidence is accumulated monotonically until either sufficient support for a boundary decision is obtained or inference is terminated due to loss of discriminative power.

Importantly, inference is not guaranteed to produce a confident decision. The solver is explicitly designed to tolerate abstention when local evidence becomes insufficient, reflecting an intrinsic limit of per-read inference rather than algorithmic failure.

7.2 Matrix-linear scoring formulation

Local evidence at each position is quantified using a deterministic matrix-linear scoring rule. For a read with bases $\{b_0, b_1, \dots, b_{L-1}\}$, cumulative evidence at position p is computed as

$$E(p) = \sum_{i=1}^p \mathbf{M}[b_{i-1}, b_i] + \mathbf{H} \cdot \mathbf{c}_p + w_{\text{pos}} \cdot p + b_0, \quad (1)$$

where \mathbf{M} is a fixed 5×5 nucleotide transition matrix, \mathbf{c}_p denotes cumulative base counts up to position p , \mathbf{H} is a vector of history weights, w_{pos} is a weak positional bias, and b_0 is a global bias term.

The transition matrix captures short-range kinetic texture characteristic of Adaptaise tailing, while the history term aggregates compositional context without introducing an explicit length prior. The bias terms regularize aggregation to ensure stable behavior under weak or noisy evidence. No individual component is interpreted in isolation; inference emerges from cumulative aggregation.

The matrix-linear formulation can be viewed as a distilled and noise-regularized representation of an underlying discrete decision process. Rather than optimizing a policy directly, Y-Trim embeds local transitions into a continuous evidence landscape, yielding stable behavior under long-tailed stochastic regimes. No component of the matrix-linear score is optimized, trained, or interpreted as a probabilistic model; it functions solely as a fixed aggregation rule for deterministic evidence accumulation under a specified sequencing chemistry.

7.3 Stopping, patience, and abstention

Inference proceeds until cumulative evidence exceeds zero, indicating sufficient support for a boundary decision. To prevent premature termination due to local fluctuations, a debounced stopping mechanism governed by a patience parameter is applied. By default, patience is set to one, allowing transient negative contributions to be absorbed.

If cumulative evidence fails to cross the decision threshold within the inference horizon, the solver explicitly abstains from deterministic placement. This outcome reflects the collapse of discriminative information at the read level and does not imply absence of tailing at the population level.

7.4 Inference horizon and information truncation

All R2 inference is constrained to a maximum horizon of $L_{\text{max}} = 25$ bases. This bound does not represent an estimate of true tail length. Instead, it reflects the rapid decay of marginal information under post-bisulfite chemistry as compositional contrast collapses.

The history-dependent aggregation term and the imposed inference horizon arise from the same underlying constraint: while population-level aggregation may reveal long-tailed distributions, additional positions beyond this range do not contribute actionable evidence at the level of individual reads. Extending inference beyond this regime would encourage exploitation of expectation-level regularities rather than read-specific signals.

Accordingly, L_{max} enforces a hard truncation once inference becomes entropy-dominated, preventing false precision and ensuring bounded computation.

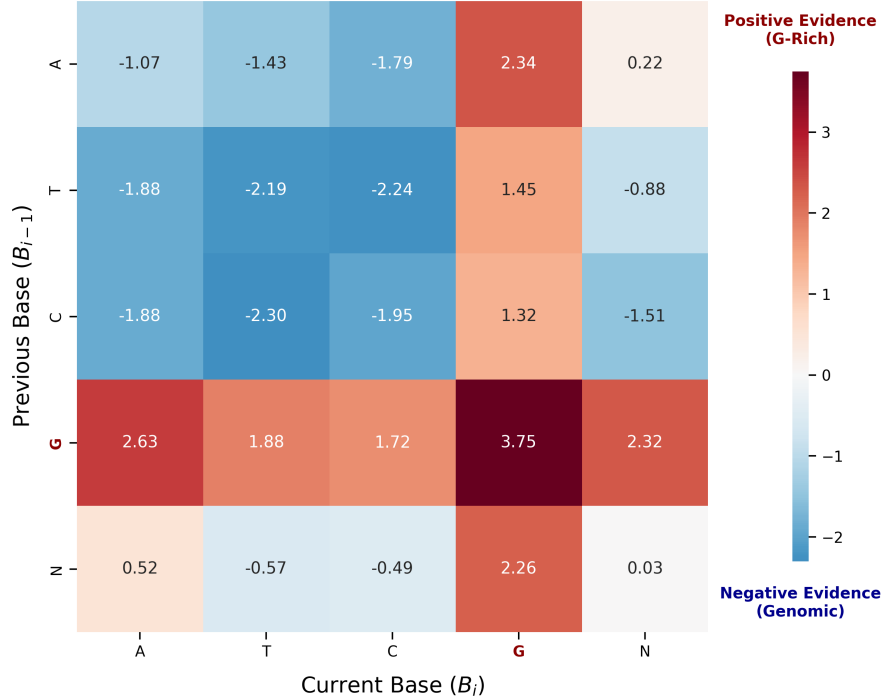


Fig. S2 Asymmetric transition structure underlying R2 boundary evidence. The transition matrix assigns positive evidence to guanine-enriched transitions characteristic of Adaptase tailing and negative evidence to transitions typical of bisulfite-converted genomic background. This asymmetry enables discrimination based on local nucleotide texture rather than absolute position or tail-length assumptions.

7.5 Parameter specification

All parameters governing R2 inference are fixed per chemistry and summarized in Table S3. These parameters define the deployed decision rule and are not tuned on evaluation data.

8 Supplementary Note 4: Conservative Projection under Inference Breakdown

This Supplementary Note formalizes the conservative projection mechanism used by Y-Trim when deterministic Read 2 boundary inference reaches its intrinsic limit. No new sources of evidence, alternative models, or performance claims are introduced. Instead, this Note specifies how unresolved uncertainty is handled in a bounded, reproducible, and chemistry-consistent manner once per-read inference ceases to be informative.

Table S2 Core parameters governing deterministic Read 2 boundary inference.

Category	Parameter	Value / Definition
Evidence aggregation	Global bias (b_0)	0.5720
	Positional weight (w_{pos})	0.0624
	History weight A	0.0072
	History weight C	-0.1183
	History weight G	0.1261
Inference control	Maximum horizon (L_{max})	25 bp
	Admission window (L_{PBSC})	30 bp
	Patience	1
	Abstention on failure	Enabled

Only nucleotide sequence content is used as input. All parameters are fixed per chemistry and remain unchanged across samples.

Throughout, projection is treated as an *operational safeguard* rather than an inferential procedure. Its purpose is to prevent forced boundary placement in entropy-dominated regimes, while preserving consistency with the decision logic applied to separable reads.

8.1 Why projection is necessary

As established in Supplementary Note 5, per-read boundary inference under post-bisulfite ssWGBS chemistry is subject to an irreducible information limit. Even when strong kinetic texture is present at early positions, cumulative evidence eventually degrades as compositional contrast collapses toward genomic background.

Deterministic inference therefore admits two qualitatively distinct outcomes. In separable reads, cumulative evidence exceeds the decision threshold within the inference horizon, yielding a confident stopping point. In non-separable reads, cumulative evidence fails to cross the threshold before the scan limit is reached. This outcome does not indicate algorithmic failure; it reflects the absence of sufficient local information to justify point-wise boundary placement.

Projection is introduced to handle the latter case. Rather than extending inference beyond the admissible window or forcing a threshold crossing, Y-Trim explicitly acknowledges inference breakdown and projects unresolved elongation behavior onto a bounded decision space.

8.2 Projection as a post-inference operation

Projection is applied *only after* deterministic inference terminates without a confident stopping decision. It does not modify the scoring function, transition matrix, positional weights, or stopping rules described in Supplementary Note 7. No additional evidence is introduced.

Operationally, projection acts on the cumulative score trajectory already computed during inference. Its role is to select a conservative representative position within the

inference horizon when point estimation is no longer supported. Importantly, projection does not recover confidence or refine the boundary estimate; it merely prevents arbitrary or overly aggressive trimming under uncertainty.

In this sense, projection is not a secondary inference step. It is a bounded response to inference exhaustion.

8.3 Projection modes

Y-Trim implements two projection modes. The deployed configuration uses a conservative composite mode (`smart`), while a fully geometric alternative (`elbow`) is provided for completeness.

smart projection (default).

In `smart` mode, projection first checks whether the cumulative score trajectory attains a non-zero maximum within the inference horizon. If such a maximum exists, the corresponding position is selected as the projected boundary. This choice reflects the strongest local evidence observed prior to inference exhaustion and is computationally inexpensive.

If the maximum cumulative score is zero, indicating uniformly weak or flat evidence, `smart` mode falls back to a geometric elbow criterion. This fallback avoids selecting positions dominated by early stochastic jitter and provides a stable projection under flat or noisy trajectories.

elbow projection.

In `elbow` mode, projection is determined exclusively by a geometric elbow criterion applied to the cumulative score trajectory. The elbow identifies the transition from initial score accumulation to saturation and serves as a conservative representative position when no clear maximum is present.

The elbow criterion operates purely on the geometry of the score trajectory. It does not introduce additional parameters, does not alter the inference process, and is computed in a single pass over the score sequence. As such, elbow-based projection reflects a structural property of the accumulated evidence rather than a secondary optimization objective.

8.4 Relationship to chemistry and tail-length variability

Projection behavior is closely tied to the long-tailed variability of enzymatic extension under Adaptase-based chemistries. Across samples, the frequency with which projection is triggered correlates with the prevalence of extended or heterogeneous tailing regimes, rather than with genomic composition differences.

Importantly, projection is chemistry-aware but not chemistry-specific. While different Adaptase formulations may alter the distribution of tail lengths, the projection mechanism itself does not change. Its role is to bound decisions once inference becomes entropy-dominated, regardless of the precise kinetic regime.

Table S3 Operational projection modes used by Y-Trim when Read 2 inference exhausts without a confident stopping point.

Mode	Operational behavior
<code>smart</code> (default)	Select max score if $\max(E) \neq 0$, otherwise apply elbow
<code>elbow</code>	Always apply geometric elbow criterion

Note. Projection modes do not modify inference parameters or scoring logic. They operate solely on the cumulative score trajectory produced during deterministic inference.

8.5 Operational modes

Operational projection is implemented via two discrete modes summarized in Table S4. The default configuration uses `smart`, with `elbow` provided as a fully geometric alternative.

8.6 Scope and non-goals

This Supplementary Note defines how Y-Trim behaves when deterministic Read 2 inference becomes non-informative. It does not evaluate projection performance, compare projection frequencies across datasets, or visualize projection behavior. Such empirical analyses are reported separately in scenario-based evaluations.

Projection is designed to be conservative by construction. Its purpose is not to maximize trimming accuracy, but to prevent the amplification of uncertainty through forced preprocessing decisions.

9 Supplementary Note 5: Read 1 Data-Driven Anchoring

9.1 Problem framing and anchoring objective

Read 1 contamination in ssWGBS arises conditionally through geometry-driven read-through, rather than through a localized enzymatic transition. As a result, per-read boundary inference for Read 1 is ill-posed on average: synthetic and genomic sequence are not reliably separable at the level of individual molecules, and observable signals become coherent only under aggregation.

Accordingly, Y-Trim formulates Read 1 handling as a *sample-level anchoring problem* rather than a per-read inference task. The goal is to determine a single, stable trimming constant for each sample that mitigates residual synthetic signal while avoiding unnecessary loss of genomic material. This objective is naturally expressed as a trade-off between *purity* (suppression of residual contamination) and *retention* (preservation of usable genomic sequence), rather than as point-wise boundary recovery.

The Read 1 anchoring procedure therefore operates exclusively on aggregate statistics derived from raw sequencing output and produces a single anchored trim length per sample. No attempt is made to localize boundaries on individual reads.

9.2 Anchoring solution overview and search space

The Read 1 anchoring solution follows a constrained search-and-score paradigm. Candidate trim lengths are evaluated within a bounded search space using baseline-referenced purity and retention scores, and the final anchored constant is selected by maximizing a combined utility function.

Table S4 Overview of the Read 1 data-driven anchoring solution.

Component	Role	Key property
Sampling	PBSC estimation	Random, non-intervening
Search space	Candidate trim lengths	Bounded (≤ 25 bp)
Direction	Anchoring direction	Read tail
Reference frame	Clean vs. polluted baseline	Data-driven
Objective	Trade-off resolution	Purity vs. retention
Decision output	Anchored trim length	One per sample

Note. This table summarizes the conceptual structure of the Read 1 anchoring solution. The search space is intentionally bounded to prevent extrapolation into regions where marginal information gain is negligible relative to compositional noise and platform drift. All components operate at the sample level and do not alter read-level randomness.

The anchoring search space is restricted to the first 25 bases from the read tail. This bound is not an estimate of the true extent of read-through, but a conservative limit beyond which additional positional context contributes diminishing information due to compositional convergence and platform-level instability. Stabilization constraints applied within this space are described in Section 9.4.

9.3 Reference baseline construction

Anchoring decisions are evaluated relative to a reference baseline that represents expected genomic composition in the absence of read-through contamination. Baseline construction defines *where* statistics are collected, not *how* decisions are made.

For Read 1, the clean baseline is extracted from an interior region of the read, chosen to be sufficiently distant from the tail while avoiding platform-dependent composition drift observed near the read end. When baseline extraction is not feasible, a predefined fallback is used.

The choice of a 25 bp offset reflects the default assumption that direct tail effects have dissipated beyond this position. A 50 bp window provides sufficient statistical stability without oversampling, while the $0.6\times$ length cap avoids late-cycle sequencing artifacts that manifest as global compositional drift, particularly in Read 1 PBSC profiles.

9.4 Purity–retention scoring and anchoring decision

For each candidate trim length t within the search space, Y-Trim evaluates two complementary quantities.

Table S5 Baseline extraction strategy and constraints for Read 1 anchoring.

Aspect	Definition
Baseline start position	25 bp from read tail
Maximum window size	50 bp
Upper bound	$\leq 0.6 \times$ read length
Rationale	Avoid tail influence and platform drift
Failure handling	Fallback baseline (defined elsewhere)

Note. Baseline parameters specify the region used for statistical reference. They do not encode trimming decisions and are independent of the anchoring objective. Fallback baselines are applied only when extraction fails due to insufficient read length or lack of valid bases.

Purity quantifies residual deviation from the pollution baseline after trimming, penalizing retained synthetic signal. *Retention* quantifies the fraction of genomic sequence preserved after trimming. Both quantities are computed at the sample level and normalized across the search space to avoid scale dependence.

Table S6 Scoring components and anchoring rule for Read 1.

Component	Definition	Normalization
Purity(t)	Deviation from pollution baseline	Min–max over t
Retention(t)	Remaining length fraction	Min–max over t
Combination	$S(t) = P(t)^\alpha R(t)^{1-\alpha}$	$\alpha = 0.5$
Selection	Anchored trim length	$\arg \max_t S(t)$
Masking	Small- t suppression	Minimum trim = 2 bp

Note. Purity and retention are evaluated independently and combined multiplicatively as a scale-free utility score. Normalization is performed per sample across the evaluated search space. Small trim lengths are masked to prevent platform-level fluctuations from dominating the decision.

The weighting parameter α is fixed to 0.5 for Read 1, reflecting a conservative bias toward retention under ambiguity. This value is not tuned per sample and does not constitute a user-facing parameter.

Anchoring uses the maximum of the combined score $S(t)$ rather than an elbow-based criterion. In Read 1, compositional contrast is weaker and score trajectories are more susceptible to broad fluctuations; selecting the global maximum yields more stable behavior across samples. Elbow-based strategies are therefore not used for Read 1 anchoring.

9.5 Stabilization constraints and practical safeguards

Two stabilization constraints are applied to ensure robust anchoring under weak or noisy evidence.

First, candidate trim lengths below 2 bp are explicitly masked. This prevents transient fluctuations at the extreme read end from dominating the anchoring decision, a behavior observed across sequencing platforms.

Second, the anchoring search is strictly bounded to the first 25 bp. Beyond this region, incremental gains in purity are negligible relative to the loss of retention, and score trajectories become increasingly dominated by noise rather than informative structure.

These safeguards are intrinsic components of the anchoring procedure and are not exposed as tuning knobs.

9.6 Relation to fixed trimming heuristics

Conventional fixed-length trimming externalizes uncertainty by requiring users to specify a constant without direct reference to sample-specific evidence. In contrast, data-driven anchoring internalizes uncertainty by selecting a constant that optimizes an explicit purity–retention trade-off under observed composition.

The anchored constant produced by Y-Trim is therefore an output of the inference process rather than an input parameter. This distinction allows trimming decisions to adapt across samples while remaining interpretable and reproducible.

10 Supplementary Note 6: Deployment, Controls, and Practical Scope

This Supplementary Note documents deployment-related considerations for Y-Trim, including the scope of user-facing controls, pipeline integration, and chemistry-specific preparation. It does not introduce additional inference mechanisms or evaluation claims, and should be read as operational context rather than algorithmic extension.

10.1 Positioning within sequencing pipelines

Y-Trim is designed to operate as an intermediate preprocessing step, positioned after basic FASTQ-level hygiene and prior to alignment. It assumes that adapter removal, gross quality filtering, and exclusion of degenerate reads (e.g., empty or extremely short sequences) have already been performed by upstream tools.

In practice, this upstream hygiene is typically handled by standard adapter and quality preprocessing tools. Y-Trim is intentionally scoped to operate after such generic FASTQ-level cleanup but before alignment. For context, widely used preprocessors such as Cutadapt exemplify this class of upstream hygiene tools, though Y-Trim does not depend on any specific implementation. [8] Similarly, modern all-in-one FASTQ preprocessors may bundle adapter trimming and basic quality filtering as a front-end step. Our analysis assumes that such generic preprocessing has already been applied and remains agnostic to the particular upstream tool used. [22]

Importantly, Y-Trim does not depend on read-pair merging, insert reconstruction, or alignment-derived information. Trimming decisions are made independently for each read based solely on observable sequence content, ensuring that behavior is invariant to pipeline ordering choices such as pre- or post-merge trimming. This design

avoids feedback loops in which trimming decisions depend on downstream artifacts introduced by alignment or merging heuristics.

Base quality scores are intentionally excluded from decision-making. Quality encodings vary across platforms and lack a consistent probabilistic interpretation under bisulfite conversion. Instead, ambiguous or degraded signal is handled explicitly through nucleotide content (including N), while coarse quality screening remains the responsibility of upstream preprocessing.

10.2 Deployment controls and operating-point semantics

The framework exposes a small number of deployment-level controls that allow users to express downstream preferences under irreducible uncertainty, without altering the underlying inference logic. These controls are intentionally limited in scope and are not intended as tuning knobs for performance optimization.

Throughout this section, we distinguish between parameters that define the inference geometry and those that merely select an operating point within an already constrained decision surface. Only the latter are exposed for routine use.

10.2.1 Trade-off parameter α

The trade-off parameter α controls the relative emphasis between purity and retention in constant-length anchoring. In the deployed configuration, α is fixed to 0.5 for Read 1, reflecting a symmetric treatment of over-trimming and under-trimming risks under geometry-limited uncertainty.

During development, we explored alternative α settings, including the application of constant anchoring to Read 2. While such configurations are technically feasible, we do not recommend deploying constant anchoring on Read 2 in routine workflows. This assessment is consistent with the Read 2 frontier analysis, where constant trimming occupies an unfavorable region of the purity–retention surface relative to inference-based solutions.

For completeness, and solely to document development-time exploration, if constant anchoring on Read 2 is nevertheless required for compatibility reasons, an exploratory reference value of $\alpha = 0.7$ may be used. This setting favors purity over retention, acknowledging the more pronounced contamination signal in Read 2. We emphasize that this value is provided as a reference from development-time exploration rather than as a recommended deployment setting.

Importantly, α is not intended to be adjusted per sample or per dataset. Changing α modifies the geometry of the decision surface itself, rather than selecting among admissible outcomes, and therefore falls outside the scope of routine deployment.

10.2.2 Offset as operating-point selection

In contrast to α , the offset parameter provides a controlled means of selecting an operating point along the existing purity–retention frontier. The offset applies a uniform shift to the final trimming position after inference or anchoring has been completed, without modifying evidence evaluation or stopping behavior.

The default offset is set to 1 base, providing a conservative balance between residual synthetic signal and unnecessary loss of genomic sequence. An offset of 0 favors maximal retention, while larger offsets increasingly favor purity. These choices do not improve inference confidence; they express downstream risk preference under known ambiguity.

The effects of offset selection are illustrated in the CpG-specific stress analysis and in scenario-based evaluation on CCGB-34. Routine offset tuning is not required, and extensive adjustment is discouraged.

10.3 Chemistry-specific preparation and parameter stability

Y-Trim is designed to operate with a fixed parameterization once the sequencing chemistry is specified. All inference rules, scoring components, and stopping safeguards are intended to remain unchanged across samples generated under the same chemistry.

During development, chemistry-specific preparation is performed offline to derive a stable, discrete scoring rule. This preparation step is not part of runtime inference and does not introduce sample-level adaptivity. In practice, this ensures that deployment cost is dominated by trimming itself rather than by parameter estimation or optimization.

The present work focuses on a single Adaptase-based ssWGBS chemistry. While alternative chemistries would require corresponding preparation, this process is performed once per chemistry and does not scale with dataset size. The details of preparation and offline rule specification are beyond the scope of this study and do not affect the interpretation of trimming behavior reported here.

10.4 Scope, non-goals, and user expectations

Y-Trim is not intended to infer physical tail length, to recover exact molecular boundaries, or to provide per-read confidence guarantees in regimes dominated by compositional ambiguity. Its goal is to enforce principled restraint: acting only where evidence supports intervention and making uncertainty explicit where it cannot be resolved.

Exposed controls are deliberately limited. Users are not expected to tune parameters extensively, and most workflows should rely on default settings. When known ambiguity exists, offset selection provides a transparent means of expressing downstream tolerance, while leaving inference unchanged.

Accordingly, deployment controls do not expand the decision space; they make explicit which decisions remain under user discretion and which are constrained by the limits of the data.

For users who intentionally depart from the default configuration—for example, by modifying rescue logic, scoring structure, or developing chemistry-specific extensions—real data alone no longer provides unambiguous feedback. In such cases, simulator-based self-checks (Supplementary Note 11) offer a controlled means of validating inference behavior under known ground truth, without altering the intended scope of routine deployment.

11 Supplementary Note 7: Simulator-Based Stress Protocols for OOD and CpG Risk

Supplementary Note 7 situates Y-Trim’s inference behavior within a simulator-backed stress framework designed to probe controlled uncertainty rather than empirical performance. Because per-read trimming boundaries are intrinsically ambiguous in post-bisulfite ssWGBS data, direct label-available read-level validation on real datasets is necessarily incomplete. We therefore evaluate inference behavior using a minimal generative simulator that exposes latent ground truth while deliberately decoupling the chemistry-typed baseline composition from tail-length structure.

This Note covers two complementary stress protocols. First, out-of-distribution (OOD) stress evaluates robustness under structural perturbations that violate assumptions used during rule preparation. Second, CpG-motivated stress examines how early trimming decisions propagate into biologically amplified downstream risk, providing an interpretable operating-point perspective on deployment choices. Together, these analyses characterize where inference remains stable, where it becomes conservative, and how residual uncertainty should be interpreted in practice.

11.1 Simulator overview and role in development-time validation

This Note describes the simulator-backed stress protocol used to evaluate inference behavior under controlled uncertainty, including out-of-distribution (OOD) regimes and CpG-motivated evaluation settings. The simulator is not intended to emulate any full sequencing workflow. Instead, it provides a minimal generative environment with explicit latent structure so that per-read boundary labels are available for analysis even when exact boundary localization is intrinsically ill-posed in real post-bisulfite ssWGBS data.

Why a simulator is necessary.

Read trimming operates at the per-read level, yet per-read ground truth boundaries are not directly observable in real data without circularity (if a reliable label existed, the trimming problem would be solved). Moreover, the most important failure regimes in this work are not “model failures” but *information-limited regimes* where multiple explanations remain statistically plausible at the single-read level (Supplementary Note 5). The simulator resolves this practical bottleneck by generating reads from an explicit concatenation of a genomic segment and an artifactual prefix while retaining the latent contamination length and boundary location as ground truth for each read.

What the simulator does (and does not) claim.

The simulator captures only the distributional ingredients that matter for trimming decisions: (i) clean genomic base composition, (ii) artifactual base composition (chemistry-typed), and (iii) a contamination-length random variable that controls how much artifactual sequence is present. It does not attempt to reproduce platform-specific error profiles, alignment artifacts, or full library-prep kinetics. Accordingly,

Table S7 Simulator components and fixed constraints used in OOD and CpG stress protocols.

Component	Symbol	Specification
Clean baseline composition	—	Bisulfite-converted genomic background (Table S8)
Pollution baseline composition	—	Chemistry-typed artifactual composition (Table S8)
Contamination length	L_{contam}	Integer RV; family specified per stress regime (see Sections 11.2–11.3)
Inference horizon	L_{max}	Fixed to 25; truncation applied to L_{contam}
Read length	L_{read}	Fixed and shared within a regime; $L_{\text{read}} \geq L_{\text{max}}$
Optional noise injection	—	Development-only (not used in OOD/CpG evaluation regimes)

Note. The simulator is designed to expose controlled structure and ground truth for read-level analysis. In the OOD and CpG protocols reported in this Note, “noise” is not injected as a separate process; stress is realized through regime shifts in contamination-length structure and chemistry-typed pollution composition (Sections 11.2–11.3).

simulation results are interpreted as *behavioral sanity checks* and stress tests, not as performance claims on real datasets.

Conceptual contribution.

This simulator provides a general development-time validation pattern for problems where read-level decisions are required but read-level labels are fundamentally ambiguous in observational data. By separating an explicit data-generating process (with ground truth) from the decision rule being evaluated, it enables controlled stress along targeted axes (tail-length structure, composition overlap, and regime shifts) without leaking real-data outcomes into rule design.

11.1.1 Generative components and fixed constraints

The simulator is composed of orthogonal components whose combination defines a synthetic regime. Each component corresponds to a distinct physical or informational factor relevant to trimming behavior and can be configured independently.

Two global constraints are enforced throughout. First, simulated contamination lengths are truncated to a fixed *analysis horizon* $L_{\text{max}} = 25$, which defines the maximum region over which per-read boundary inference is treated as operationally meaningful in this work. Second, Read 2 simulations assume a fixed read length sufficient to represent the full analysis horizon ($L_{\text{read}} \geq L_{\text{max}}$). The analysis horizon is identical to the inference horizon defined in Supplementary Note 7; the terminology is adapted here to emphasize its role as a standardized coverage window for simulator-based stress evaluation rather than as a parameter inferred from data.

11.1.2 Baseline composition models (chemistry-typed)

Baseline compositions specify the nucleotide statistics of (i) clean, post-bisulfite genomic sequence and (ii) chemistry-typed synthetic contamination. They define the *chemical reference frame* of the stress protocols. By construction, baseline sets are

Table S8 Chemistry-typed baseline composition models used in simulator-based protocols.

Set	Read	State	Type	A	C	G	T	N
D	R2	Clean	Empirical (dev)	0.500	0.275	0.015	0.205	0.005
	R1	Clean	Complement (dev)	0.205	0.015	0.275	0.500	0.005
	R2	Pollution	Adaptase head (dev)	0.185	0.010	0.785	0.010	0.010
	R1	Pollution	Read-through (dev)	0.230	0.085	0.250	0.425	0.010
E	R2	Clean	De-noised genomic	0.50	0.27	0.02	0.21	0.00
	R2	Pollution	De-noised Adaptase (dominant-G)	0.20	0.00	0.80	0.00	0.00

Note. Set D is restricted to development/preparation and includes explicit N mass. Optional position-dependent N injection (if used) is development-only and applied post hoc, after baseline sampling. Set E omits explicit N mass and is used for evaluation-oriented stress protocols (OOD and CpG), applied to Read 2 only. Contamination-length distribution families for L_{contam} are defined per protocol in Sections 11.2 (OOD) and 11.3 (CpG).

chemistry-dependent but *distribution-independent*: the same baselines can be paired with different contamination-length families to serve different objectives (development, OOD stress, CpG stress).

We use two baseline sets with distinct roles. Set D is used for development-time preparation and robustness probing under explicitly degraded inputs. Set E is used for evaluation-oriented stress (OOD and CpG) and reflects typical post-filtering libraries with de-noised composition (no explicit N mass). Reporting these baselines supports protocol reproducibility and does not constitute a realism claim about any particular platform.

Set D (development / preparation).

Set D is used during rule preparation and internal stress probing. It includes an explicit N mass term to emulate degraded inputs and to prevent decision rules from implicitly relying on unrealistic cleanliness. In addition, development runs may optionally apply a mild position-dependent N injection near read termini as a worst-case instability stress; this is a development-only perturbation applied *after* baseline sampling and is not part of the evaluation protocols.

Set E (evaluation / OOD / CpG).

Set E is used for evaluation-oriented stress protocols (OOD and CpG). It omits explicit N mass and uses a chemistry-typed dominant-G contamination composition, consistent with the dominant-G regimes analyzed in this work. All OOD and CpG configurations in this Note use Set E and are applied to Read 2 only.

11.1.3 Contamination-length distributions as task-dependent stressors

Contamination-length distributions define the *structural uncertainty* presented to the inference framework, independently of chemical composition. While baseline compositions are chemistry-typed and fixed for a given evaluation regime, the choice of contamination-length family determines the nature of the stress being applied.

In this Note, we intentionally decouple baseline specification from distributional choice. The same chemistry-typed baselines (Set E; Table S8) are paired with different L_{contam} families to probe distinct failure modes: structure-free ambiguity, multi-scale mixtures, long-tail bias, and chemistry-specific shifts. Accordingly, contamination-length distributions are defined and justified within each evaluation protocol (Sections 11.2 and 11.3), rather than at the simulator definition level.

On protocol-specific sample sizes.

Simulation sample sizes depend on the objective of each stress protocol (e.g., stabilizing distributional shape versus estimating risk-sensitive endpoints). Accordingly, sample sizes are reported within each evaluation subsection (Sections 11.2–11.3), rather than in the simulator definition.

11.2 Out-of-distribution (OOD) stress evaluation

Out-of-distribution (OOD) stress is used to evaluate inference behavior under structural perturbations that violate assumptions implicit in rule preparation. Unlike development-time simulation, which emphasizes smooth and unbiased regimes for rule derivation, OOD evaluation deliberately introduces mismatched or adversarial contamination-length structures to probe robustness.

In this setting, the objective is not pointwise recovery of true trimming boundaries, which is ill-defined under intrinsic ambiguity, but stability of inferred trimming distributions and preservation of chemical consistency.

11.2.1 Evaluation criteria and OOD distribution families

OOD evaluation prioritizes two interpretable criteria: (i) agreement at the *distributional level* between inferred trimming profiles and simulated boundary distributions, and (ii) preservation of per-base sequence content (PBSC) after trimming. These criteria reflect the intended behavior under uncertainty: conservative adaptation rather than forced resolution.

During development, rule preparation used a smooth unimodal reference surface for L_{contam} to stabilize offline exploration. In contrast, OOD stress replaces this assumption with alternative families that intentionally remove or distort positional structure. Each OOD regime is evaluated using 2,000 simulated reads, which is sufficient to stabilize distributional shape without introducing unnecessary sampling variance.

11.2.2 Rationale for OOD stress design

The OOD distributions are not intended to approximate realistic tail-length statistics. Instead, each is constructed to expose a distinct *behavioral risk* that can arise when inference assumptions are violated. The focus is on observable failure modes rather than on internal algorithmic mechanisms. In particular, numeric choices (e.g., the reference center near 8 and the analysis horizon $L_{\text{max}} = 25$) are used as *coverage parameters* to define a standardized stress surface. They should not be interpreted as assumed truth about the physical tail-length distribution.

Table S9 Contamination-length distribution families used for out-of-distribution (OOD) stress. All samplers produce an integer contamination length L_{contam} and are truncated to the inference horizon $[0, L_{\text{max}}]$ with $L_{\text{max}} = 25$.

Family	Sampler definition	Role
Normal (dev reference)	$L_{\text{contam}} \sim \mathcal{N}(\mu=8, \sigma^2=8^2)$ (rounded; truncated)	Reference location-scale surface (development only)
Uniform	$L_{\text{contam}} \sim \text{UnifInt}(0, 25)$	OOD stress
Bimodal	$\begin{cases} \mathcal{N}(5, 1^2) & \text{w.p. 0.5} \\ \mathcal{N}(20, 1^2) & \text{w.p. 0.5} \end{cases}$ (rounded; truncated)	OOD stress
Long-tail	$L_{\text{contam}} \sim \mathcal{N}(16, 4^2)$ (rounded; truncated)	OOD stress
Poisson	$L_{\text{contam}} \sim \text{Poisson}(\lambda=8)$ (truncated)	OOD stress

Note. All OOD configurations use the de-noised baseline set (Set E; Table S8) and are applied to Read 2 only. The Gaussian family is used exclusively during development and is not part of OOD evaluation. The reference Normal family is used only to provide a smooth location-scale stress surface centered near empirically reported tail extents. For context, fixed-length trimming remains a common pragmatic default in bisulfite-seq workflows (e.g., the widely used Trim Galore! wrapper), motivating our focus on stress-testing inference behavior against heuristic-style assumptions rather than claiming realism of any single generative family. [9]

Specifically, the location parameter $\mu = 8$ is chosen to fall near the scale of synthetic tail extents reported in later vendor documentation [7], and serves solely to center a broad coverage window rather than to represent a fitted or assumed tail-length distribution.

Table S10 Out-of-distribution (OOD) stress regimes and targeted behavioral risks.

Distribution	Challenge
Uniform	Absence of positional structure (overfitting risk)
Bimodal	Mixture-induced ambiguity (mode instability)
Long-tail	Positional distributional shift (transfer failure)
Poisson	Minor shift from development prior (sensitivity test)

By framing OOD stress in terms of observable phenomena and associated risks, this design tests whether inference behavior remains stable and conservative under assumption violations, without privileging any specific generative model.

11.3 CpG-motivated stress and operating-point interpretation

11.3.1 Why CpG-dense contexts amplify early trimming errors

Unlike OOD stress, which probes robustness under structurally mismatched tail-length regimes, CpG-motivated evaluation targets a downstream *risk amplifier*: CpG-dense regions convert small 5' compositional perturbations into disproportionate methylation bias. Consequently, position-wise comparisons can be misleading: a method may appear locally competitive at a handful of early bases while remaining unstable in aggregate. We therefore evaluate behavior through a 5'-weighted risk aggregation that emphasizes early positions, where ssWGBS boundary ambiguity and biochemical consequences are both maximal.

Table S11 Components of the CpG-weighted 5'-end risk aggregation.

Component	Definition	Rationale
Baseline	Genomic G background level	Reference for excess signal
Excess term	$\max(0, G(p) - G_{\text{bg}})$	Prevent depletion from canceling risk
Position weights	$\exp(-\lambda p)$, $\lambda = 0.3$, $p \in [0, 20]$	Focus on early 5'-end instability
Aggregation	Weighted sum over window	Integrated CpG-sensitive risk

Note. The aggregation window is restricted to the first 20 bases to reflect the region where CpG-associated risk amplification is strongest; parameters are fixed across all CpG evaluations.

11.3.2 CpG simulator configuration and risk aggregation

CpG stress uses the de-noised, chemistry-typed baselines (Set E; Table S8) and is applied to Read 2 only. To construct a boundary regime that makes CpG-weighted risk non-degenerate, contamination lengths are sampled from a shifted Poisson family,

$$L_{\text{contam}} = 1 + X, \quad X \sim \text{Poisson}(\lambda=8),$$

followed by truncation to the analysis horizon $[0, L_{\text{max}}]$ with $L_{\text{max}} = 25$. The +1 shift is an *operational conditioning proxy* rather than a mechanistic claim: it enforces the presence of a minimal artifactual prefix so that early-position risk is evaluated in the regime where trimming decisions are actually relevant, and avoids the degenerate “all-clean” case ($L_{\text{contam}}=0$) that would otherwise dominate risk aggregation under a pure Poisson model. Numeric choices here (e.g., $\lambda=8$ and $L_{\text{max}}=25$) define a standardized stress surface and do not constitute a fitted model of real tail-length statistics.

This conditioning is used purely to avoid the degenerate all-clean case and to ensure the stress target is non-trivial. However, we do not treat the shifted model as an identifiable description of library formation. Its role is to define a controlled stress surface for operating-point interpretation, while empirical context for tail behavior and rescue-triggered regimes is described separately in Supplementary Notes 12–13.

Because CpG evaluation aggregates risk over positions rather than stabilizing only distributional shape, we use a larger simulation sample size ($N = 50,000$ reads) to reduce Monte Carlo variance in the integrated endpoint.

11.3.3 Interpreting offset as an operating-point selector under CpG risk

CpG evaluation also provides a natural setting to interpret the deployment offset as an *operating-point selector*. Importantly, offset does not modify the underlying inference rule; it selects among a small set of post-inference operating points that trade residual artifact suppression against avoidable composition distortion.

In CpG-dense contexts, this distinction matters because the most visually salient PBSC features need not correspond to the most biologically appropriate operating point. For example, an offset of 0 can produce apparent early “cleanliness” via local depletion of guanine, a pattern that may arise from unavoidable texture-driven preferences of any per-read decision rule operating in a heterogeneous and partially

indistinguishable regime. Such depletion should not be interpreted as evidence that the read is biologically clean; it is a consequence of conservative stopping under limited discriminative information.

We therefore use offset = +1 as the recommended default operating point in CpG-facing settings: it reduces the risk of offset-dependent depletion patterns and provides a more balanced expression of the retention–purity trade-off under aggregation. Offset = +2 represents a more aggressive choice for users who prioritize additional suppression of residual guanine-rich signal and are willing to accept the corresponding retention cost. These operating-point interpretations are consistent with the frontier view developed on real data: multiple offsets trace distinct points on a fixed inference frontier, enabling practical navigation without re-deriving the decision rule.

12 Supplementary Note 8: CCGB-34 Benchmark and Scenario-Based Evaluation

This Supplementary Note documents the real-data evaluation framework used to contextualize the deployment behavior of Y-Trim under realistic ssWGBS conditions. Unlike the simulator-based stress protocols described in Supplementary Note 11, which isolate specific distributional and chemical factors under controlled generative assumptions, the CCGB-34 suite operates entirely on observational sequencing data and therefore reflects substantial real-world complexity of library preparation, insert-length geometry, and biochemical variability encountered in practice.

The goal of this Note is not primarily to establish a leaderboard-style benchmark, nor to claim ground-truth boundary recovery on real data, which is fundamentally unobservable at the per-read level. Instead, CCGB-34 is constructed as a *structured evaluation surface* that exposes how trimming behavior evolves across coherent signal regimes, including clean controls, canonical Adaptase kinetics, geometry-limited projection, benign but adversarial early-position fluctuations, and negative-control protocols (non-Adaptase libraries).

Evaluation on CCGB-34 emphasizes three deployment-relevant questions. First, does a method activate trimming only when chemically and geometrically supported, and abstain otherwise? Second, when trimming is activated, how does behavior trade retained genomic sequence against residual artifactual signal? Third, are these trade-offs stable across heterogeneous real-world scenarios, or do they collapse under regime shifts that are common in ssWGBS data?

Throughout this Note, CCGB-34 is treated as a scenario-indexed assessment surface rather than as a collection of independent samples. Interpretation focuses on consistency, abstention behavior, and trade-off structure, rather than on absolute dominance or aggregate accuracy. All reported analyses are aligned with the deployment model described in the main text and Supplementary Note 10, and are intended to clarify how design choices manifest under realistic operating conditions.

12.1 CCGB-34 as a structured evaluation surface

CCGB-34 is designed as a *structured evaluation surface* rather than a leaderboard-style benchmark. Its purpose is not to rank trimming strategies by peak performance, but

to expose how activation, abstention, and trade-off behavior evolve across qualitatively distinct ssWGBS regimes that arise in practice.

Unlike simulator-backed protocols (Supplementary Note 11), CCGB-34 operates entirely on real sequencing data and therefore reflects the full complexity of library preparation, insert-length geometry, and biochemical variability. At the same time, CCGB-34 is curated to preserve *scenario structure*: runs are grouped at the project (SRP) level, and each group represents a coherent physical or chemical regime rather than independent samples.

How to read CCGB-34.

Table S12 provides a *scenario-level map* of the suite: seven SRP-level groups (G1–G7), each intentionally chosen to isolate a distinct source of uncertainty relevant to trimming. Table S13 provides the corresponding *SRR-level manifest* used in this study, including per-run annotations that support traceability (e.g., the 7 bp trap, longitudinal pairs, and cases where Read 1 is unassessable due to extremely short effective read-through). Because Table S13 is large, it may appear later in the Supplement; however, all CCGB-34 results in this Note reference groups and runs exactly as listed in Tables S12 and S13.

Coverage across regimes.

At a high level, CCGB-34 spans four evaluation roles (Table S12). (i) *Clean or negative controls* (G6, and the clean/trap structure in G5) test specificity and over-activation, including non-Adaptase protocols where trimming should abstain. (ii) *Canonical Adaptase kinetics* on Read 2 (G2–G4) represent the primary deployment regime in which post-gating read-level inference is meaningful. (iii) *Geometry-limited feasibility* on Read 1 (notably G1 and subsets of G2/G4) stresses feasibility constraints imposed by cfDNA fragmentation and conditional read-through. (iv) *Non-enzymatic early-position fluctuation* (G5 and G7) provides benign but adversarial PBSC patterns that can trigger false activation if chemistry is misinterpreted.

Why this is not a single-number benchmark.

CCGB-34 is evaluated in a trade-off space rather than by a scalar accuracy. Across groups, the dominant failure modes differ: some regimes require abstention to preserve specificity (e.g., non-Adaptase controls), while others require navigating an intrinsic retention–purity trade-off under Read 2 ambiguity. Accordingly, CCGB-34 is treated as a scenario-indexed assessment surface in which interpretation emphasizes consistency, abstention behavior, and frontier structure, rather than absolute dominance.

12.2 CCGB-34 assessment protocol: activation, abstention, and frontier metrics

CCGB-34 evaluation is organized as a two-stage protocol: an activation layer that determines when read-level trimming is warranted, followed by a trade-off assessment on activated samples using two complementary frontier axes. This structure mirrors

Table S12 Scenario-level structure of the CCGB-34 evaluation surface. Each group (G1–G7) represents a distinct stress regime rather than a comparative benchmark. Groups are constructed to isolate specific physical or chemical failure modes in ssWGBS, including Geometry-limited read-through, enzymatic tailing kinetics, non-enzymatic early-position fluctuation, and negative-control conditions without Adaptase chemistry.

Group	SRP	Species	Context	Signal regime
G1	SRP325062 ^b	H. sapiens	CSF cfDNA (extreme fragmentation)	R1: Geometry-limited read-through R2: Weak / minimal kinetic signal
G2	SRP619043 ^c	H. sapiens	ALS plasma cfDNA	R1: Severe geometric truncation ^a R2: Canonical Adaptase tailing
G3	SRP299418 ^d	H. sapiens	Plasma cfDNA (variable input depth)	R1: Minimal geometric distortion R2: Canonical Adaptase tailing
G4	SRP475142 ^e	M. musculus	Pancreas LCM (low input)	R1: Mild geometric lift R2: Canonical Adaptase tailing
G5	SRP533334 ^f	H. sapiens	Nasal swab	R1: No geometric artifact R2: Early-position fluctuation (non-enzymatic); Includes 7 bp trap
G6	SRP636882 ^g	H. sapiens	Heart cfDNA (NEBNext)	R1: No geometric artifact R2: No enzymatic signature (non-Adaptase negative control)
G7	SRP620537 ^h	H. sapiens	Lung FFPE (KAPA)	R1: No geometric artifact R2: Chemical noise; Early-position stochasticity

Note. Signal regimes are reported descriptively to characterize the dominant source of uncertainty in each group. Read 1 is treated as a feasibility constraint rather than a performance axis, reflecting its geometry-limited nature in post-BS ssWGBS.

^a In a subset of runs, Read 1 is unassessable due to extremely short effective read-through (≈ 9 bp), and is therefore excluded from per-read inference by design.

^b Source study for G1 (SRP325062): [11].

^c Source study for G2 (SRP619043): [12].

^d Source study for G3 (SRP299418): [13].

^e Source study for G4 (SRP475142): [14].

^f Source study for G5 (SRP533334): [15].

^g Source study for G6 (SRP636882): [16].

^h Source study for G7 (SRP620537): [17].

the deployment philosophy of Y-Trim: abstain when chemistry evidence is absent or ambiguous, and evaluate trimming quality only when trimming is actually invoked.

12.2.1 Sample-level activation and abstention

Activation is reported explicitly because abstention is itself a primary outcome on CCGB-34: several CCGB groups are designed to test *non-activation* (negative controls) or geometry-limited feasibility (Read 1), rather than to reward aggressive

Table S1.3 Detailed SRR-level manifest of CCG-B-34 (34 runs). Each SRR corresponds to one scenario group (G1–G7). Entries document per-run context and dominant signal characteristics for traceability, rather than serving as independent evaluation units. Annotations flag longitudinal pairs, a known 7 bp genomic fluctuation trap, and cases where Read 1 is unassessable due to extremely short effective read-through.

Group	SRP	SRR	Context within SRR	R1	R2	Notes
G1	SRP325062	SRR14879169	Low throughput	Dirty	Clean	R2 appears pre-trimmed (weak R2 signature)
G1	SRP325062	SRR14879181	Low Input 1	Dirty	Clean	R2 appears pre-trimmed (weak R2 signature)
G1	SRP325062	SRR14879183	Low Input 2	Dirty	Clean	R2 appears pre-trimmed (weak R2 signature)
G1	SRP325062	SRR14879186	Medium 1	Dirty	Clean	R2 appears pre-trimmed (weak R2 signature)
G1	SRP325062	SRR14879188	Medium 2	Dirty	Clean	R2 appears pre-trimmed (weak R2 signature)
G2	SRP619043	SRR35337269	Age 57y	Dirty	Dirty	
G2	SRP619043	SRR35337272	Age 65y, high depth	Dirty	Dirty	
G2	SRP619043	SRR35337279	Age 42y	Dirty	Dirty	
G2	SRP619043	SRR35337297	Age 71y, low depth	N/A	Dirty	R1 unassessable ($\approx 9\text{bp}$)
G2	SRP619043	SRR35337306	Age 80y	N/A	Dirty	R1 unassessable ($\approx 9\text{bp}$)
G3	SRP299418	SRR13308049	Elderly (Age 80)	Clean	Dirty	
G3	SRP299418	SRR13308053	Extreme low input	Clean	Dirty	Longitudinal pair (descriptor only)
G3	SRP299418	SRR13308056	Patient 5, D15	Clean	Dirty	Longitudinal pair (descriptor only)
G3	SRP299418	SRR13308068	Patient 5, D0	Clean	Dirty	Longitudinal pair (descriptor only)
G3	SRP299418	SRR13308088	High depth anchor	Clean	Dirty	
G4	SRP475142	SRR27002286	Normal duct	Dirty	Dirty	
G4	SRP475142	SRR27002287	Normal acinar	Dirty	Dirty	
G4	SRP475142	SRR27002297	Caerulein D4	Dirty	Dirty	
G4	SRP475142	SRR27002302	ADM1 D2	Dirty	Dirty	
G4	SRP475142	SRR27002322	Panc_AK_D2	Dirty	Dirty	
G5	SRP533334	SRR30711033	Severe, Male 66y	Clean	Clean	7bp genomic fluctuation trap; 7bp trap sample (no enzymatic tailing)
G5	SRP533334	SRR30711056	Mild, Female 77y	Clean	Clean	
G5	SRP533334	SRR30711057	Severe, Female 69y	Clean	Clean	
G5	SRP533334	SRR30711058	Mild, Male 41y	Clean	Clean	
G5	SRP533334	SRR30711060	Severe, Male 28y	Clean	Clean	
G6	SRP636882	SRR35954090	LA-CM_6	Clean	Clean	Non-Adaptase protocol (NEBNext)
G6	SRP636882	SRR35954091	LA-CM_5	Clean	Clean	Non-Adaptase protocol (NEBNext)
G6	SRP636882	SRR35954093	LA-CM_8	Clean	Clean	Non-Adaptase protocol (NEBNext)
G6	SRP636882	SRR35954094	LA-CM_7	Clean	Clean	Non-Adaptase protocol (NEBNext)
G7	SRP620537	SRR35407494	LUAD, 100bp	Clean	Clean	FFPE chemical noise; early-position stochasticity
G7	SRP620537	SRR35407500	LUAD, high depth	Clean	Clean	FFPE chemical noise; early-position stochasticity
G7	SRP620537	SRR35407502	SCLC, 100bp	Clean	Clean	FFPE chemical noise; early-position stochasticity
G7	SRP620537	SRR35407509	Control, 150bp	Clean	Clean	FFPE chemical noise; early-position stochasticity
G7	SRP620537	SRR35407519	SCLC, high depth	Clean	Clean	FFPE chemical noise; early-position stochasticity

Note. SRR-level annotations are descriptive and are not used as evaluation axes. Longitudinal pairs are included to illustrate internal consistency within a scenario group, but are not analyzed as temporal trajectories. Where detectable, “R2 appears pre-trimmed” is recorded as a cohort descriptor (indicating weak or minimal Adaptase kinetic signal), not as an algorithmic outcome. R1 activation frequency varies across geometry-driven groups but is not interpreted as a performance metric. Source studies for each SRR are listed in Table S12.

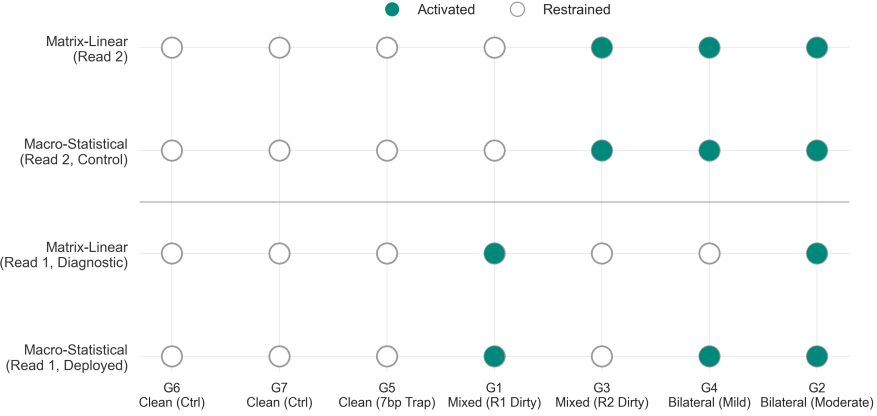


Fig. S3 Activation and abstention frequency across CCGB-34 scenarios. The panel reports the fraction of samples in which trimming is activated, stratified by read and by inference variant. CCGB-34 includes regimes designed to reward abstention (negative controls and non-kinetic early-position fluctuation) as well as regimes where Read 2 carries canonical Adaptase evidence. The diversity of abstention patterns—including cases where Read 1 adaptive variants abstain while a constant-cut baseline trims—supports the interpretation that activation is a first-class decision layer, not merely an implementation detail.

trimming. Accordingly, the activation panel is shown with four rows rather than two: in addition to the deployed Read 2 inference branch, we include development-time variants to illustrate how abstention behavior changes when inference structure is weakened or when constant-cut heuristics are forced. These development-only variants are shown solely to illustrate how abstention changes when inference structure is intentionally weakened; they are not used for any primary conclusions.

A key example is Read 1 behavior in the mouse low-input regime (G4). Although G4 is described at the scenario level as exhibiting a mild Read 1 geometric lift (Table S12), adaptive Read 1 handling may abstain globally on CCGB-34 when the aggregate evidence is insufficient, while a constant-cut heuristic can still force trimming. This contrast emphasizes that activation is a first-class decision layer and that non-action can be an appropriate response under geometry-limited uncertainty, consistent with the main-text interpretation.

12.2.2 Two QC-style reporting axes for CCGB-34 frontier plots

To visualize the retention–purity trade-off on real sequencing data without invoking per-read ground truth, we report two chemistry-consistent, post-cut composition summaries computed in a short window immediately after each method’s *sample-aggregated* mean cut position. These axes are not proposed as universal benchmarks and are not used to optimize any method; they serve only as a consistent coordinate system for CCGB-34 scenario plots, enabling interpretation of activation, abstention, and operating-point shifts under fixed chemistry baselines. All baselines are fixed (Set E; Table S8), and all reporting hyperparameters below are held constant across runs and across CCGB-34 groups.

Let c denote the sample-aggregated mean cut position for a method and read, and let $p = c + i$ for $i \in \{0, 1, 2, 3, 4\}$ index a short post-cut window. Let $\pi_b(p)$ be the observed per-base content at position p for base $b \in \{A, C, G, T\}$, expressed as a fraction. We use chemistry-typed genomic baselines π_b^{bg} (Table S8) and apply a conservative *clean-enough* indicator so that retention accounting is not credited in positions that still exhibit dominant synthetic signal.

12.2.3 Axis 1: retained genomic composition (proxy for avoidable over-trimming)

This axis summarizes *avoidable loss of genomic composition* immediately after the reported cut. Intuitively, it penalizes deficits of expected genomic bases in a short post-cut window, treating them as a proxy for over-trimming under the chemistry-typed reference frame.

Read 2 retained-genome score.

For Read 2, we treat low guanine as the proxy for having crossed the dominant-G synthetic region, and measure the residual deficit of genomic bases (C/T) relative to a near-cut reference:

$$\mathcal{R}_{\text{R2}}(c) = \sum_{i=0}^4 w_i \cdot \mathbf{1}[\pi_G(c+i) < \tau_{\text{R2}}] \cdot \left(\max\{0, \pi_C^{\text{ref}}(i) - \pi_C(c+i)\} + \max\{0, \pi_T^{\text{ref}}(i) - \pi_T(c+i)\} \right), \quad (2)$$

$$w_i = \frac{1}{i+1}, \quad \tau_{\text{R2}} = 0.05, \quad (3)$$

where $\pi_C^{\text{ref}}(i)$ and $\pi_T^{\text{ref}}(i)$ are light near-cut reference levels anchored to the genomic baseline (with a small tolerance at $i = 0$ to reflect inevitable boundary jitter). We report the *retained genomic bases* score as

$$\text{Retained}_{\text{R2}} = 1 - \kappa \cdot \mathcal{R}_{\text{R2}}(c), \quad (4)$$

with κ used only to place values on a comparable 0–1 plotting scale (reported as percentages in figures).

Read 1 retained-genome score.

For Read 1, the roles of bases swap under post-bisulfite structure (Supplementary Notes 5–6). We use low cytosine as the clean-enough condition and measure deficit of (G/A) relative to baseline:

$$\mathcal{R}_{\text{R1}}(c) = \sum_{i=0}^4 w_i \cdot \mathbf{1}[\pi_G(c+i) < \tau_{\text{R1}}] \cdot \left(\max\{0, \pi_G^{\text{ref}}(i) - \pi_G(c+i)\} + \max\{0, \pi_A^{\text{ref}}(i) - \pi_A(c+i)\} \right), \quad (5)$$

$$\tau_{\text{R1}} = 0.10, \quad (6)$$

and define $\text{Retained}_{\text{R1}} = 1 - \kappa \cdot \mathcal{R}_{\text{R1}}(c)$ with the same reporting convention.

12.2.4 Axis 2: residual artifact composition (proxy for under-trimming)

This axis summarizes *residual synthetic signal* retained immediately after the reported cut. It is computed over the same post-cut window and uses chemistry-consistent dominant and secondary markers as a fixed reporting convention.

Read 2 residual artifact score.

For Read 2, residual artifact is dominated by excess guanine together with a secondary depletion of adenine relative to the genomic baseline:

$$\mathcal{U}_{\text{R2}}(c) = \sum_{i=0}^4 w_i \cdot \left(0.8 \cdot \max\{0, \pi_G(c+i) - \pi_G^{\text{bg}}\} + 0.2 \cdot \max\{0, \pi_A^{\text{bg}} - \pi_A(c+i)\} \right). \quad (7)$$

Read 1 residual artifact score.

For Read 1, residual artifact is dominated by excess cytosine with secondary thymine enrichment:

$$\mathcal{U}_{\text{R1}}(c) = \sum_{i=0}^4 w_i \cdot \left(0.8 \cdot \max\{0, \pi_C(c+i) - \pi_C^{\text{bg}}\} + 0.2 \cdot \max\{0, \pi_T(c+i) - \pi_T^{\text{bg}}\} \right). \quad (8)$$

Residual artifact is reported on the same 0–1 plotting scale (percentage in figures), where lower indicates cleaner post-trim composition immediately after the inferred boundary.

Reporting scale (implementation note).

All scores are linearly rescaled to a 0–1 range for plotting convenience only; rescaling does not affect within-sample ordering and is not used for any decision-making.

12.2.5 Offset as an operating-point selector on a fixed frontier

Frontier plots in the main text visualize a family of operating points produced by a *single* inference rule. The deployment offset does not alter inference or re-train any component; instead, it shifts the reported operating cut by an integer number of bases:

$$c_{\text{deploy}} = c_{\text{infer}} + o, \quad o \in \{0, +1, +2\}, \quad (9)$$

and re-evaluates the same sample under the same chemistry baselines using the reporting axes above. Conceptually, the inference rule defines a constrained decision geometry, while the offset selects a small set of post-inference operating points that trade residual artifact suppression against avoidable composition loss.

This interpretation is important for CCGB-34 because certain local PBSC features reflect unavoidable texture-driven micro-preferences under intrinsic ambiguity rather

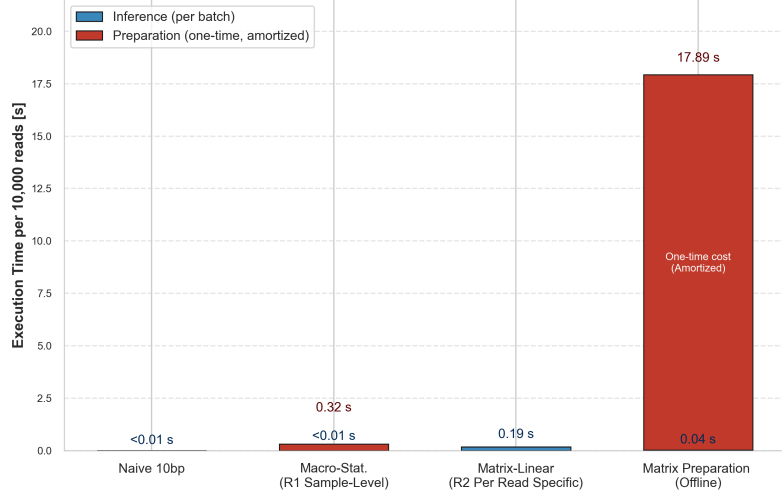


Fig. S4 Engineering efficiency and deployment cost of trimming strategies. Execution time per 10,000 reads on CPU (file I/O excluded), decomposed into **per-read trimming cost on Read 2** (blue) and **sample-level preparation cost** (red, amortized per sample). Sample-level preparation includes FASTQ sampling/PBSC aggregation, sample-level gating, and Read 1 macrostatistical anchoring; it is incurred once per sample and does not scale with read count. Per-read trimming refers exclusively to Read 2 matrix-linear boundary inference and scales linearly with the number of reads on which trimming is activated. Timing is *activation-aware*: only samples for which the corresponding method activates trimming are included; clean samples on which a method abstains incur zero trimming cost and are excluded. The final bar reports one-time, offline matrix preparation cost (per chemistry), shown separately and not incurred during deployment throughput.

than true biochemical cleanliness. Offset = +1 is used as the default because it provides the most balanced expression of the retention–purity trade-off in aggregate: it avoids interpreting local depletion patterns (often visible at $o=0$) as genuine improvement, while not incurring the additional retention cost of more aggressive settings. Offset = +2 provides an explicit option for users who prioritize additional suppression of residual dominant-G signal at the expense of retention, without changing the underlying inference frontier.

12.3 Engineering efficiency and deployment cost

Beyond biological correctness, practical deployment of trimming requires predictable, bounded computational behavior under realistic workloads. We therefore report the engineering cost of representative trimming strategies under an *activation-aware* evaluation protocol that reflects how these methods are actually used in practice.

Activation-aware timing protocol.

Execution time is measured *only* on samples for which trimming is activated under the corresponding method. Clean samples on which a method abstains incur no trimming cost and are excluded from timing, consistent with real-world deployment where trimming logic is bypassed entirely when no action is taken. This distinction is essential:

methods that aggressively trim all samples are not rewarded for unnecessary computation, and methods that abstain appropriately are not penalized for work they never perform.

All runtime benchmarks are reported per batch of 10,000 reads using a full Python implementation on CPU, with file I/O excluded to isolate algorithmic overhead. For paired-end data, only the contaminated read is timed in asymmetric cases, reflecting deployment behavior where Read 1 and Read 2 are handled independently and geometry-limited reads may be skipped entirely.

Separation of inference and preparation costs.

Figure S4 decomposes computational cost into two orthogonal components. Blue bars report *per-batch inference time*, corresponding to work performed at runtime on activated samples. Red bars report *one-time preparation cost*, incurred offline during development and amortized across all subsequent runs.

Naive fixed-length trimming and macro-statistical trimming incur negligible per-batch runtime cost. Macro-statistical trimming additionally requires a lightweight sample-level aggregation step, but this preparation is performed once per sample and does not scale with read count. In contrast, Y-Trim performs adaptive per-read inference on Read 2 using a matrix-linear scoring rule, resulting in a modest but predictable per-batch runtime overhead. Importantly, this overhead is incurred only on samples where Read 2 trimming is activated.

Offline matrix preparation.

The final column in Figure S4 reports the offline cost required to prepare the deterministic scoring matrix used by Y-Trim. This step is performed *once per chemistry* during development, does not depend on sequencing data, and is not part of the trimming pipeline. Because the resulting matrix is fixed and reused across all samples, its cost is amortized over the lifetime of a deployment and does not affect throughput.

Interpretation.

Taken together, these results illustrate a deliberate engineering separation: computationally intensive exploration and stabilization occur offline, while deployment relies on a compact, deterministic scoring rule with bounded per-read cost. The resulting runtime behavior scales linearly with the number of activated reads and remains competitive with simpler heuristics, while providing substantially richer adaptive behavior under chemically heterogeneous conditions.

13 Supplementary Note 9: Rescue behavior and long-tail contamination

This Supplementary Note examines the role of the *rescue* mechanism in Y-Trim and clarifies the statistical and engineering conditions under which rescue is activated in real ssWGBS data. Unlike the primary inference logic, which aims to infer a stable trimming boundary under typical Adaptase kinetics, rescue is designed as a controlled safety response to regimes in which boundary inference becomes intrinsically unstable.

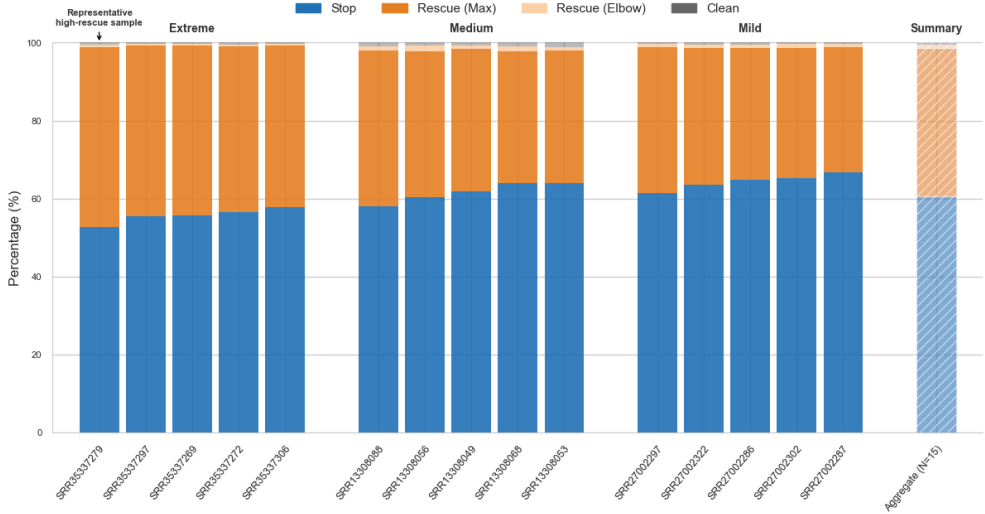


Fig. S5 Composition of decision outcomes under rescue-enabled inference across contaminated CCGB-34 Read 2 regimes. Stacked bars report the fraction of reads assigned to each terminal decision state under the deployed matrix-based inference rule: early stop (blue), rescue via maximum extension (orange), rescue via elbow criterion (light orange), and clean/no-action (gray). Samples are grouped by contamination severity (Extreme, Medium, Mild), ordered within each group by decreasing rescue trigger rate. Rescue decisions dominate in extreme regimes, while early stopping becomes progressively more prevalent as contamination weakens. A representative high-rescue sample is annotated to illustrate a library in which long-tail behavior is frequent and rescue is repeatedly required. The rightmost bar summarizes aggregate behavior across all contaminated CCGB-34 samples ($N = 15$). Importantly, rescue activation is not restricted to a narrow “failure zone” but spans a substantial fraction of reads, indicating that rescue acts as a general mechanism for handling extended or heterogeneous tail processes rather than a rare exception handler.

The analyses in this Note focus on Read 2 behavior under CCGB-34 dirty regimes, where long-tail contamination events are empirically observed. The goal is not to establish a definitive generative model for tail formation, but to characterize when single-process assumptions break down and to explain why a dedicated rescue pathway is required to preserve stable deployment behavior.

13.1 Rescue trigger frequency reflects contamination severity

We first quantify how often rescue is triggered across CCGB-34 regimes of increasing contamination severity. Rescue activation is reported as the fraction of reads within a sample for which the primary boundary inference is deemed unstable and a rescue decision is invoked.

Across CCGB-34 dirty Read 2 groups, rescue trigger rates increase monotonically from mild to medium and extreme regimes. This ordering is consistent across libraries and reflects increasing prevalence of long-tail contamination rather than differences in sequencing depth or batch effects.

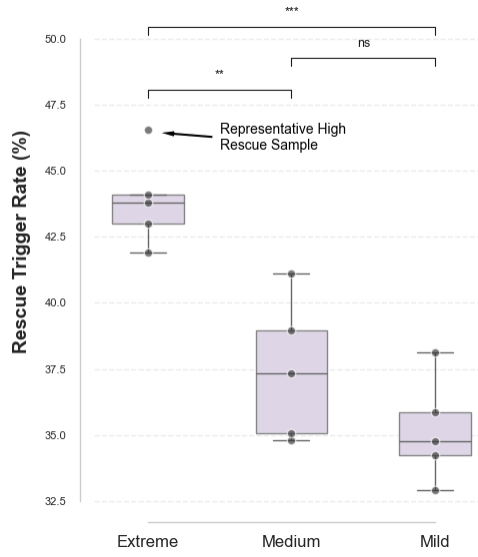


Fig. S6 Rescue trigger rate stratified by contamination severity. Boxplots show the distribution of rescue trigger rates (percentage of reads invoking either rescue mode) across CCGB-34 Read 2 contaminated samples, grouped by severity regime (Extreme, Medium, Mild). Individual libraries are overlaid as points; a representative high-rescue library is annotated. Rescue activation decreases monotonically from extreme to mild regimes, reflecting reduced prevalence of extended tail behavior. Statistical comparisons are performed using Welch's *t*-test (two-sided); significance levels are indicated above brackets. These results demonstrate that rescue engagement scales with contamination severity and is not driven by isolated outliers, supporting its role as a regime-adaptive component rather than a pathological fallback.

These results indicate that rescue is not a rare or pathological event, but a systematic response to long-tailed contamination regimes. At the same time, rescue is not uniformly applied: even in extreme regimes, a substantial fraction of reads terminate via standard early stopping, suggesting that rescue targets a specific subset of unstable reads rather than replacing boundary inference wholesale.

13.2 Rescue alters termination behavior rather than forcing trimming

To clarify how rescue affects trimming decisions, we next examine the composition of termination outcomes across contamination regimes. Each read is classified into one of four mutually exclusive categories: (i) clean termination without trimming, (ii) early stopping under standard inference, (iii) rescue termination via a maximum-bound rule, or (iv) rescue termination via an elbow-based criterion.

Across all regimes, standard early stopping remains the dominant outcome. However, the relative contribution of rescue termination increases with contamination severity, particularly in extreme regimes. This pattern indicates that rescue primarily intervenes when tail behavior deviates strongly from the assumptions underlying early stopping.

Importantly, rescue does not simply extend trimming deeper into the read. Instead, it provides an alternative termination logic that caps instability when boundary evidence becomes diffuse or overdispersed. In this sense, rescue acts as a stabilizing mechanism that limits error propagation rather than as an aggressive trimming strategy.

13.3 Failure of single-process models under long-tail contamination

To understand why rescue is preferentially activated in extreme regimes, we examined the empirical structure of tail-length distributions in representative CCGB-34 libraries spanning representative Poisson-dominant, mixed, and tail-enriched contamination profiles.

Observed distributions consistently exhibit a dominant central body together with a heavy, extended tail that becomes more pronounced as contamination severity increases. Accordingly, we use overdispersed count-family surrogates (e.g., negative-binomial-like components) purely as descriptive statistical baselines for tail mass, not as claims about identifiable biochemical mechanisms. [23] This structure is visible even when aggregation is restricted to reads that trigger rescue, indicating that rescue is associated with genuinely long-tailed events rather than random fluctuation.

While the empirical distributions can be *descriptively* approximated using a two-component representation consisting of a Poisson-like body and an overdispersed tail, enforced single-process models systematically fail to capture the observed tail mass. This failure is especially pronounced in extreme regimes, where long contamination events occur with non-negligible probability.

These observations are not intended to assert a specific generative mechanism for tail formation. Rather, they demonstrate that long-tail contamination constitutes a statistically distinct risk regime that cannot be adequately accommodated within any single-kinetic hypothesis, even when such a model is optimally fitted.

Within this context, rescue serves a clear operational role. By detecting when boundary inference enters a regime dominated by tail instability, rescue provides a controlled termination strategy that limits the impact of overdispersed contamination without requiring explicit commitment to a particular tail-generation model. This separation between inference under typical conditions and stabilization under tail-dominated conditions is essential for maintaining robust trimming behavior across heterogeneous ssWGBS datasets.

Interpretive scope.

Rescue should therefore be understood not as an alternative inference algorithm, but as a safety mechanism that enforces conservative behavior when the statistical structure of the data violates the assumptions required for stable boundary inference. Its activation patterns and outcome distributions reflect the empirical prevalence of long-tail contamination rather than any hard-coded preference for aggressive trimming.

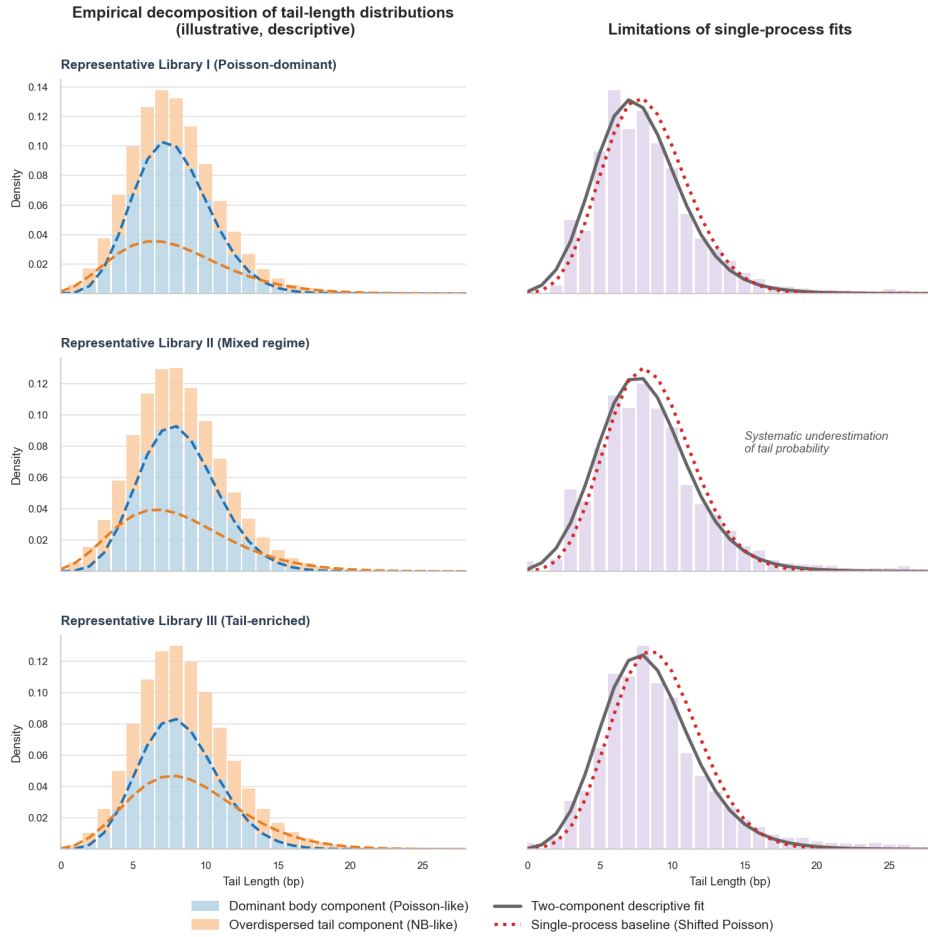


Fig. S7 Empirical tail-length decomposition and failure of single-process models. Left panels show illustrative empirical tail-length distributions from three representative libraries spanning Poisson-dominant, mixed, and tail-enriched regimes. Observed distributions (histograms) are decomposed into a dominant body component (Poisson-like; blue) and an overdispersed tail component (negative-binomial-like; orange), whose sum yields a descriptive two-component fit (gray). Right panels compare the same empirical distributions to an optimally fitted single-process baseline (shifted Poisson; red dotted). Across all regimes, single-process models systematically underestimate long-tail probability, even when body fit appears adequate. This pattern indicates that extended tail events arise from a statistically distinct stochastic contribution rather than from overdispersion within a single mechanism. The decomposition is descriptive rather than generative and is presented to motivate the need for rescue-capable inference, not to claim identifiability of latent biochemical processes.